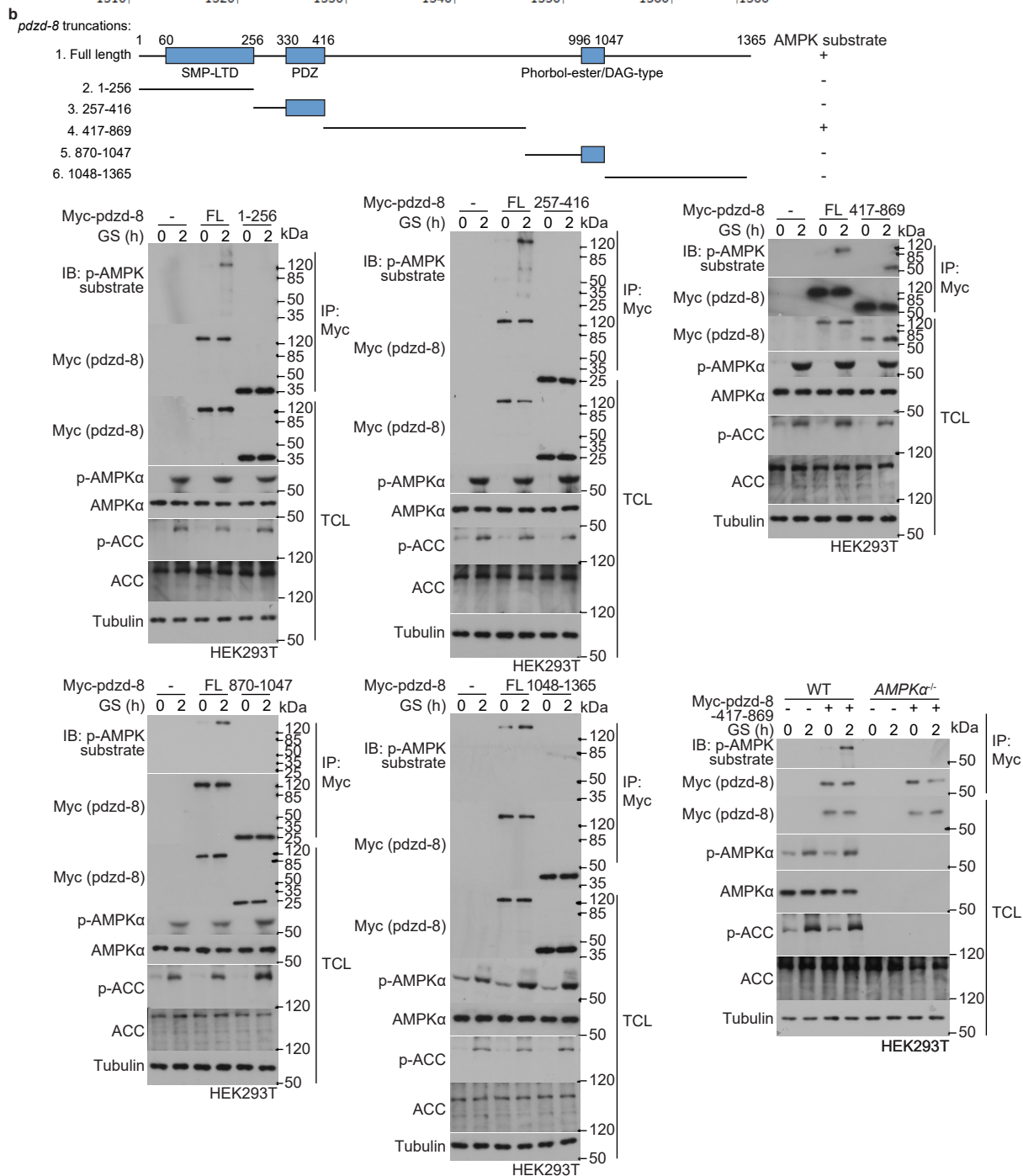


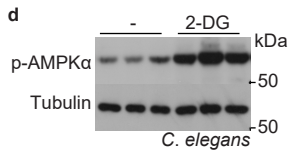
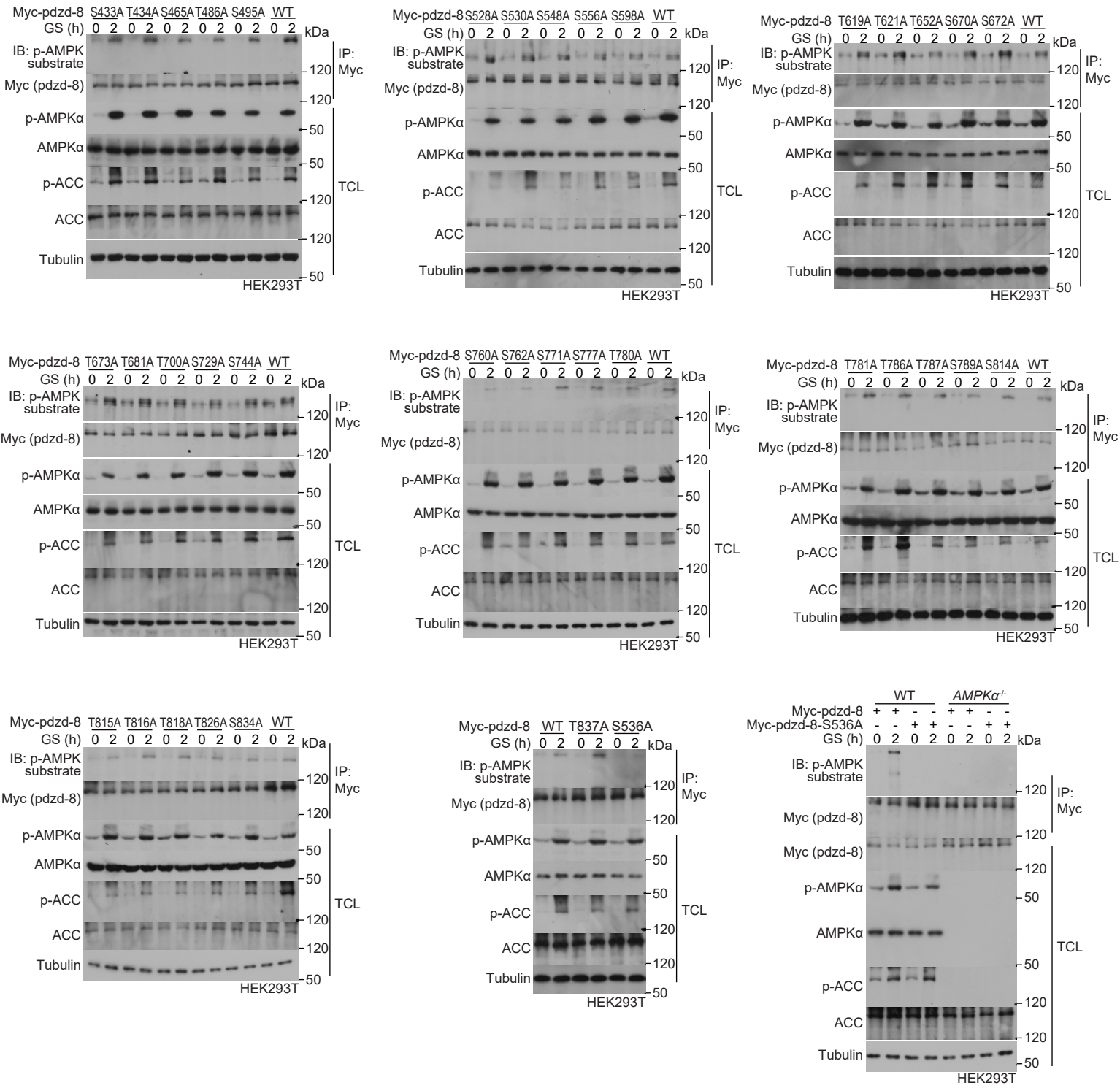
a

MLIAFLVGFICGVLLLLGILYIFIVDPWAPPTDQPQPPIEQFRPAQIPEELRTFLKSGEDGGGISKWE **SCNSISL**LLHLMFLQEHKD **TRALRRV**WHKRLQM
 1| 10| 20| 30| 40| 50| 60| 70| 80| 90| 100|
 EMNDITTRSAAGRLIQEIRREL **SLG**TKFMT **INSIRV**SEVEMADDKNT **FDK**IVFILDIDYSGGFETSIDVSTIIAKKAS **LSVKI**TKLTGMVRVILSRQPY
 110| 120| 130| 140| 150| 160| 170| 180| 190| 200|
 HHWTFSEVFSQPIFETDINSIQGHQLKRLIPIIKEAIRR **SLQR**KHWPNYKIRYRPFPPNPIFQASPPINSFTHIKMEGGIEVTVLQC **SR**LKNALLDDK
 210| 220| 230| 240| 250| 260| 270| 280| 290| 300|
 NKNEYVYCTVSIERSPIVQNEEQGHVVNVLTFSTRYDV **SSPI**GLVFDKNVAAT **GNNT**NRVAKVCT **VED**NLSLADKAAFKPGDVLVAINNVP **IR**SERQATRF
 310| 320| 330| 340| 350| 360| 370| 380| 390| 400|
 LQSTTGDLTVLVERSLDDIDEESKEAAEIV **SV**TRVDIGTGSVNDTADSTLSINNSVANDRD **SLK**DDDKTIGGIPAKDGKINAT **ALA**ARRRHSVSNLE
 410| 420| 430| 440| 450| 460| 470| 480| 490| 500|
 SSVIDTNTSEVASSIFGLDAHKFDKPP **SV**SVQRAESARVPQLISQPS **FD**LRRQT **SE**SHLDAKVIDAVLSSADFGMENSVEDEIKMLLVGDLNRSASAG
 510| 520| 530| 540| 550| 560| 570| 580| 590| 600|
 HNLDPQLLVGVKREKDK **TL**TQADASKGLALIASQTGSVASLSSMISNRDT **TG**TEDGGDDEEAHLDRKRS **AS**TRKAKIQATFAAGKKKVLDMPPQKRKNT
 610| 620| 630| 640| 650| 660| 670| 680| 690| 700|
 DASDLNGESIEIGADAGSLYDTDNRDP **SI**GRSPMAVVGKRKES **PS**DEKKEKKRLLKKL **SE**SPKIRRAAGSAQDKQSPM **TT**IKARTTKSVQFQKFDVMW
 710| 720| 730| 740| 750| 760| 770| 780| 790| 800|
 GQSLHFEFDSPPET **TT**RTVIRYLNVT **VH**AKEVKSAG **TP**TTSATNVPNATPSTPDSIASSTNTD **NS**VPTNISADSKPILLGSVSLFVLPQLIDDCRL **TL**SN
 810| 820| 830| 840| 850| 860| 870| 880| 890| 900|
 CHREVVQLKQPNTSSPQTSPDDPMLAEFARHAGYDPRLCFGDITLGFYRFPNGFPVDKAIN **SG**DESEDELNRIHNSKDVASPTRPF **SPP**ALSPASHDWK
 910| 920| 930| 940| 950| 960| 970| 980| 990| 1000|
 LWYGKNS **TT**CAMCRGKIWRNASS **SR**CLVICHNKC **VV**KANS **GG**IACTPQQLHTPPSNLQLHSDHEHFEISASELDHPSVTPGDHQIDETRSLIMQSPST
 1010| 1020| 1030| 1040| 1050| 1060| 1070| 1080| 1090| 1100|
 PSSSIAGSLDTPEMSKRARFRKVT **EK**FSNWRKGGKKKDDDDDFIGRRE **TI**DSCADTGSLSQSDISNRD **SP**MASIQDVLSDVLPGLDGSFPFISGLYFQPG
 1110| 1120| 1130| 1140| 1150| 1160| 1170| 1180| 1190| 1200|
 NAYNEQTIRNAKMLGREIFCDLPSEQRVERIN **SQ**IDRIQT **AI**RETKDNRL **SV**MQNGGDI **SE**SSAKFQGLDERLQALAVVLMHYCSALQDCQSGRST **P**APP
 1210| 1220| 1230| 1240| 1250| 1260| 1270| 1280| 1290| 1300|
 PDDDNQKRE **IT**EEISSVNVDSNNEEDSESVLDED **TV**TGDPVQHDHPLERPT **KL**DPSSDAVEAHS*
 1310| 1320| 1330| 1340| 1350| 1360| 1366|

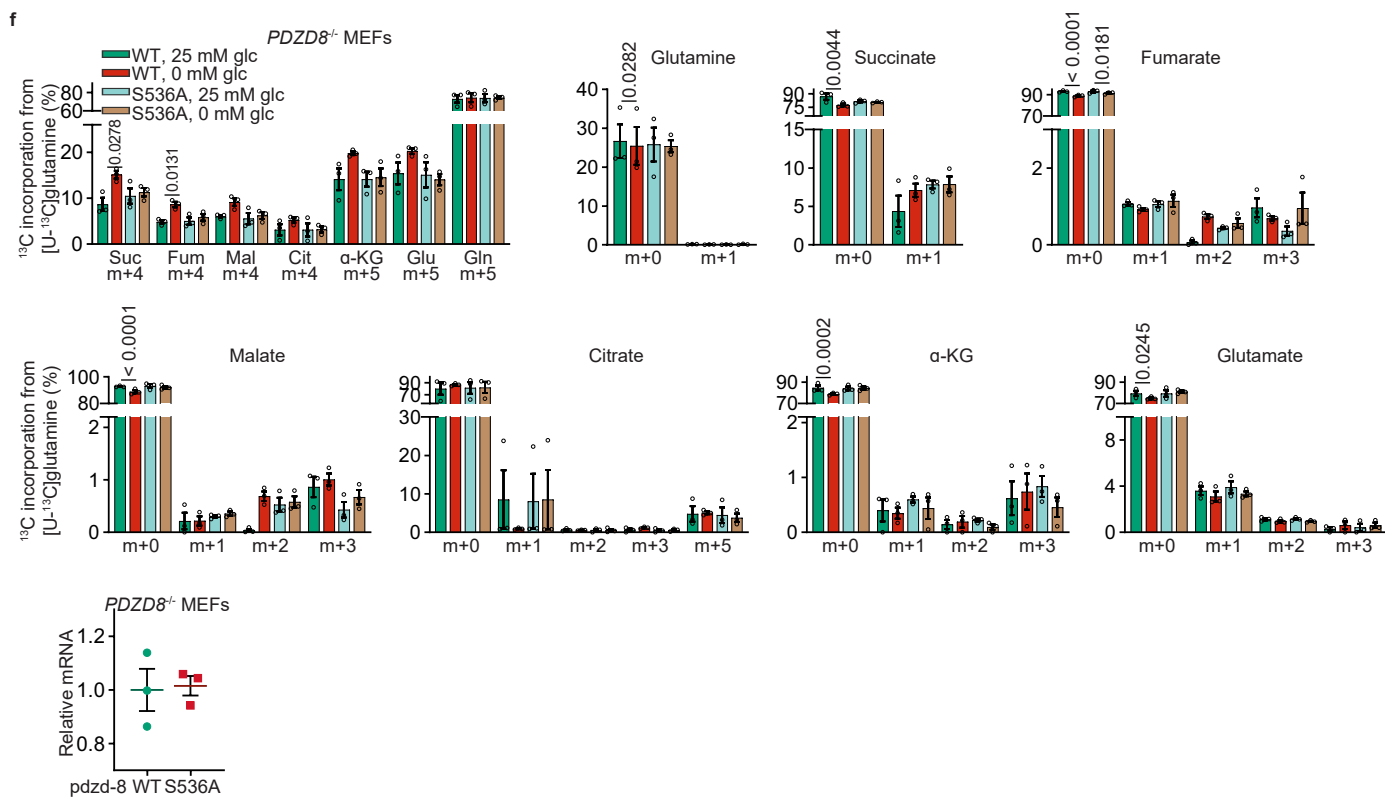
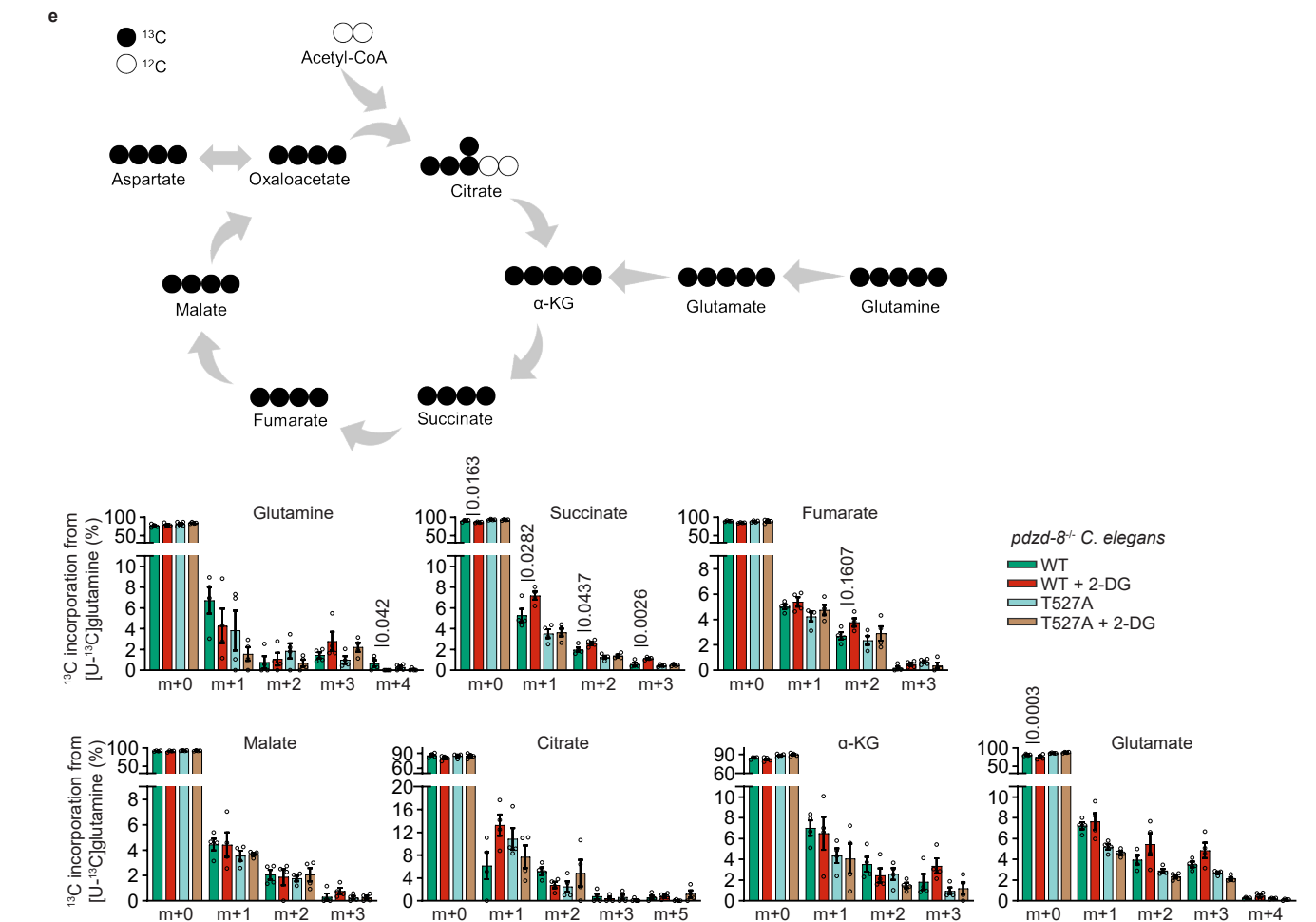


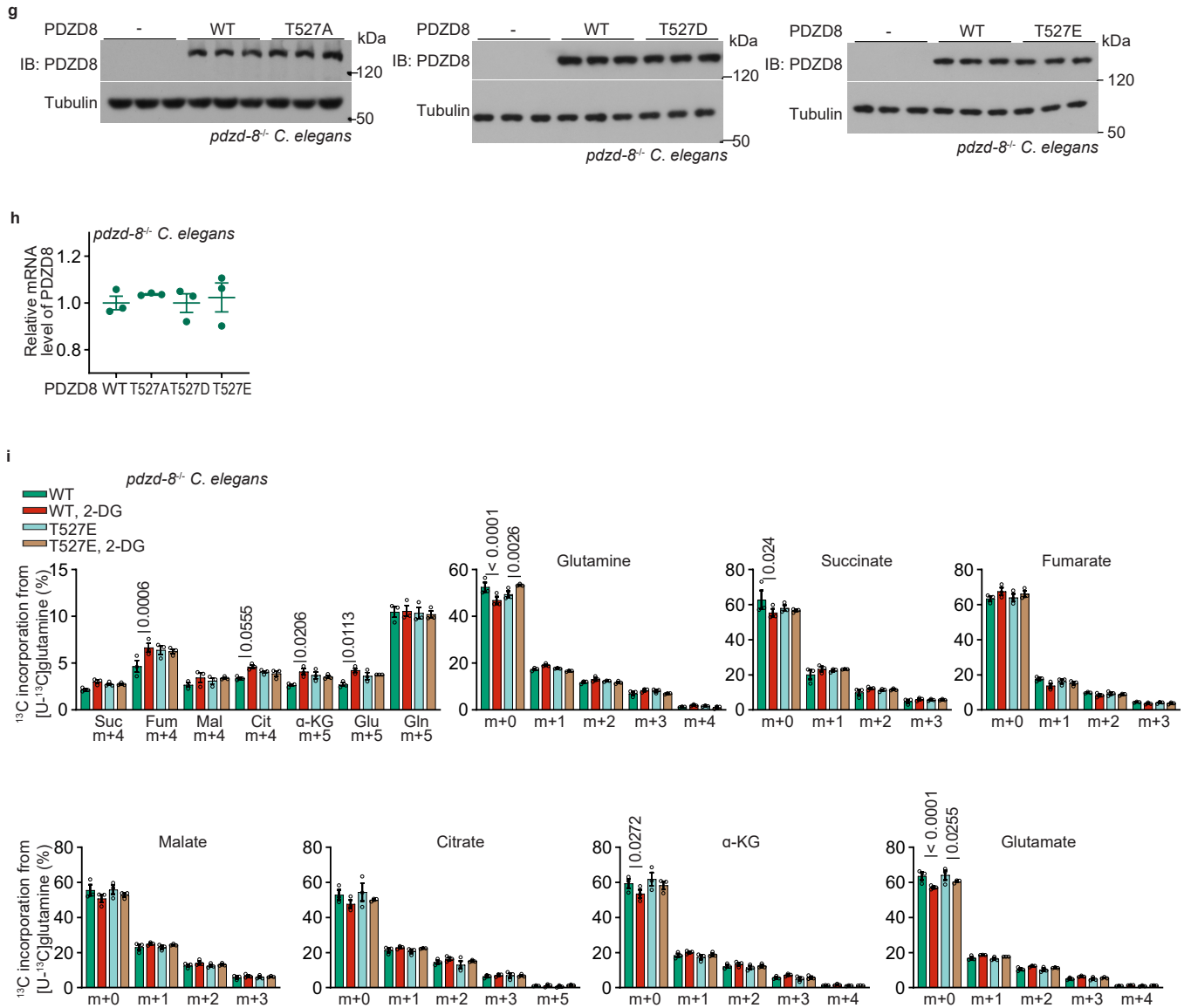
Supplementary information, Fig. S1

c



Supplementary information, Fig. S1 (Cont.)





Supplementary information, Fig. S1 Nematode AMPK-PDZD8-GLS1 axis plays a conserved role in promotion of glutaminolysis in mammalian cells.

a-c AMPK phosphorylates the S536 site of *pdzd-8* in nematodes. HEK293T cells, either wildtype or *AMPK α* ^{-/-}, were transfected with Myc-tagged *pdzd-8* (**b**, **c**), *pdzd-8* deletions (**b**), or *pdzd-8* point mutations (**c**), and then glucose-starved for 2 h. Cells were then lysed, followed by immunoprecipitation of Myc-tag and immunoblotting using the pan-phospho-AMPK-substrates antibody. See also the potential phosphoacceptor sites (colored in magenta) that fit the conserved motif of the AMPK substrates of *pdzd-8* in **a**. FL, full length.

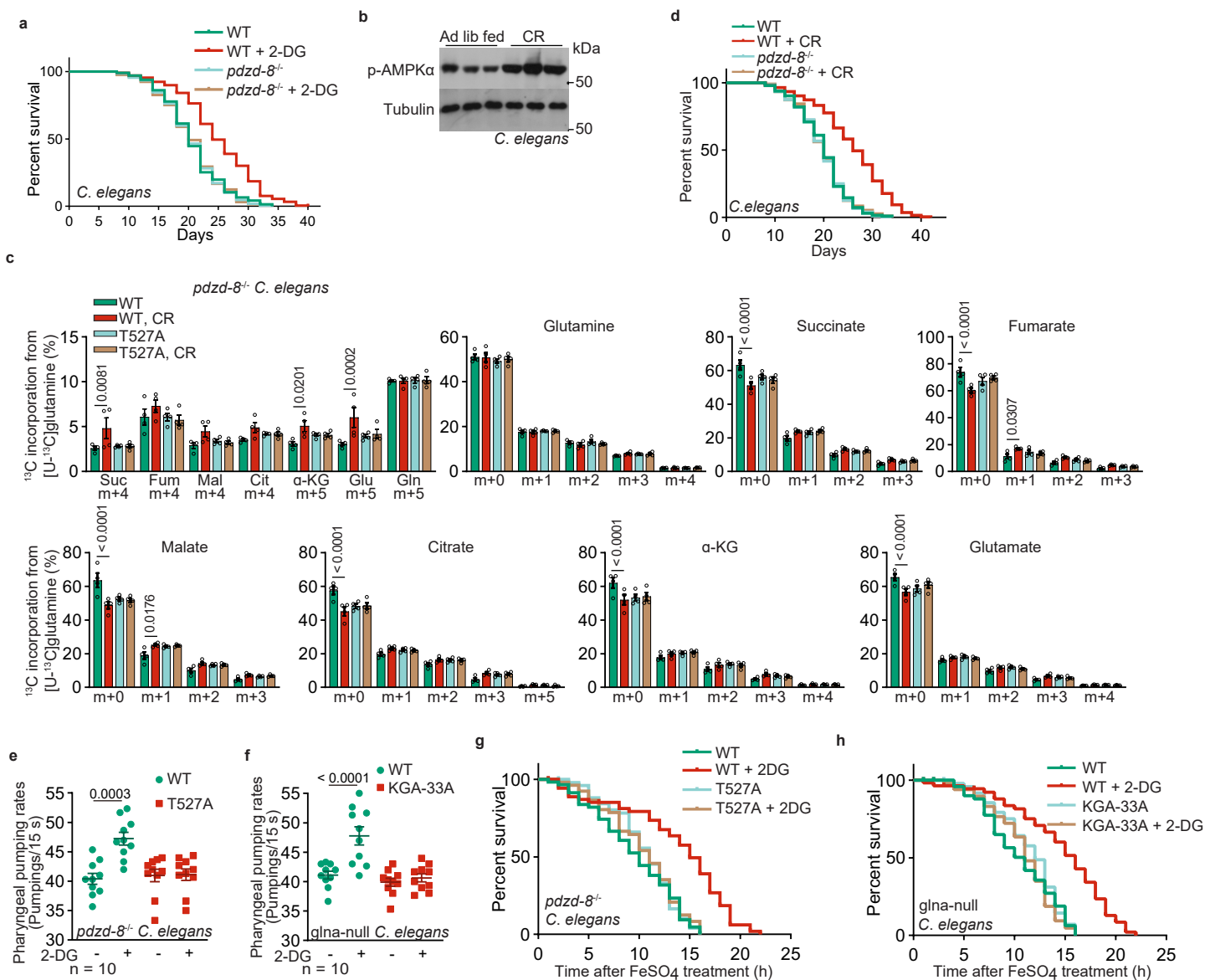
d Fasting activates nematodes AMPK. Nematodes were treated with 4 mM 2-DG that mimics fasting, for 2 days, and the AMPK (*aak-2*) phosphorylation was determined by immunoblotting.

e Human PDZD8-T527A blocks fasting-induced glutaminolysis in nematodes. The *pdzd-8*^{-/-} nematodes with re-introduced human PDZD8 or PDZD8-T527A were treated as in Fig. 1b. Data are shown as mean \pm SD; n = 4 biological replicates for each condition/genotype; p values were calculated by two-way ANOVA, followed by Tukey. Levels of other isotopomers of the labeled TCA cycle intermediates are shown in Fig. 1b.

f Nematode *pdzd-8*-S536A blocks fasting-induced glutaminolysis in mammalian cells. The *PDZD8*^{-/-} MEFs with *pdzd-8* or *pdzd-8*-S536A stably expressed (the mRNA levels of *pdzd-8* and *pdzd-8*-S536A were confirmed using RT-PCR and are shown in the lower panel as mean \pm SEM; n = 3 samples for each gene; p values were determined by two-way ANOVA) were glucose-starved for 2 h, followed by determination of glutaminolysis through analyzing the levels of labeled TCA cycle intermediates by GC-MS. Data are shown in the upper panel as mean \pm SEM; n = 4 samples for each condition. p values were determined by two-way ANOVA, followed by Tukey.

g, h Validation of the expression levels of PDZD8 and its mutant T527A, T527D, and T527E when re-introduced into *pdzd-8*^{-/-} nematodes by immunoblotting (**g**) and RT-PCR (**h**; data shown as mean \pm SEM; n = 3 samples for each gene; p values were determined by two-way ANOVA, followed by Tukey).

i PDZD8-T527E promotes glutaminolysis regardless of low glucose. Experiments were performed as in Fig. 1b, except that *pdzd-8*^{-/-} nematodes with human PDZD8-T527E mutant re-introduced were used. Data are shown as mean \pm SEM; n = 4 samples for each condition. p values were determined by two-way ANOVA, followed by Tukey. Experiments in this figure were performed three times.



Supplementary information, Fig. S2 AMPK-PDZD8-GLS1 axis exerts rejuvenating effects in nematodes

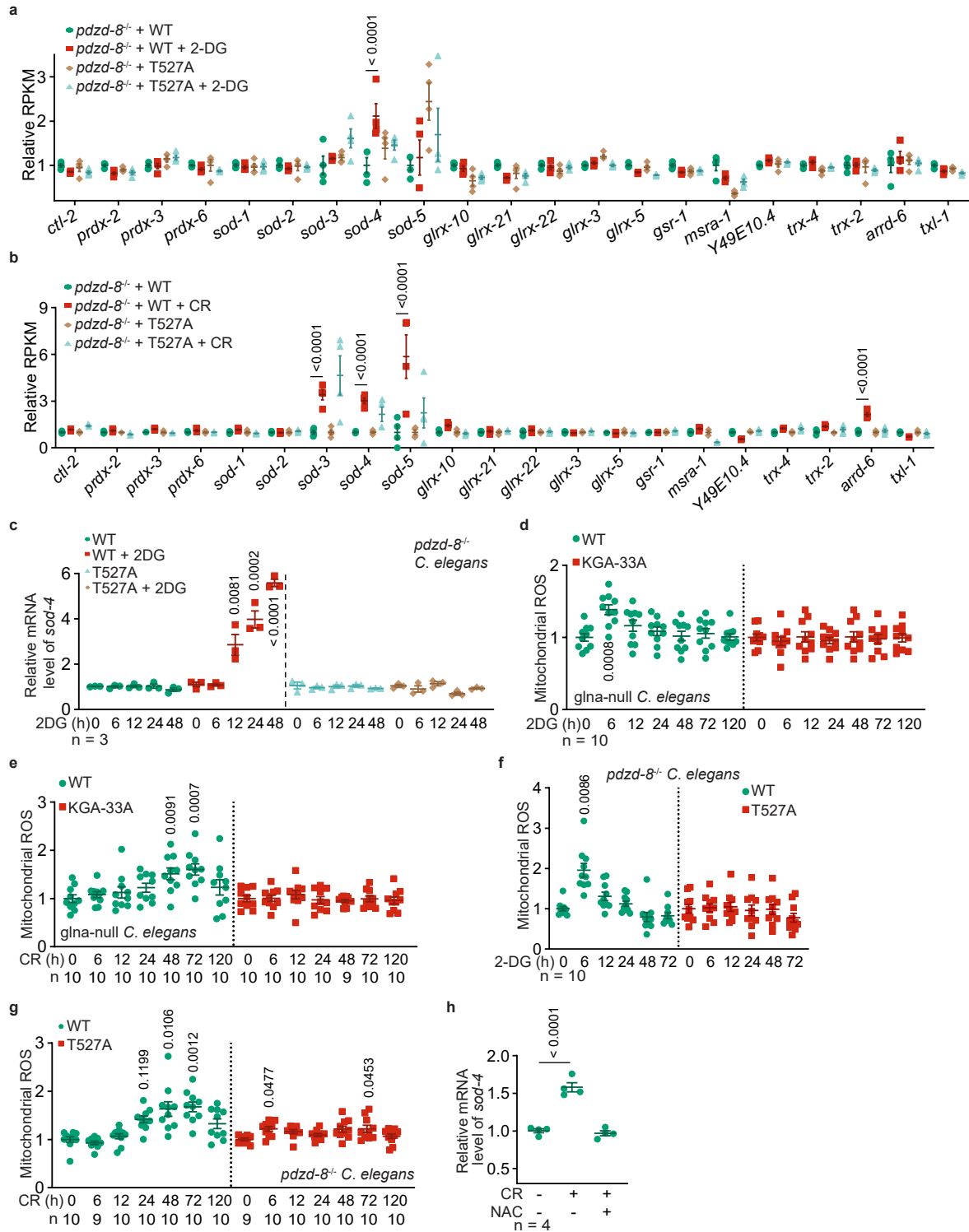
a, d PDZD8 extends the lifespan of nematodes in low glucose. The *pdzd-8^{-/-}* nematodes were treated with 2-DG (**a**) or subjected to CR (**d**). Lifespan data are shown as Kaplan-Meier curves.

b CR activates nematode AMPK. Nematodes were subjected to CR for 2 days, and the AMPK (*aak-2*) phosphorylation was determined by immunoblotting.

c PDZD8-T527A blocks CR-induced glutaminolysis in nematodes. The *pdzd-8^{-/-} C. elegans* strains with re-introduced human PDZD8 or PDZD8-T527A were subjected to CR for 2 days, followed by determination of glutaminolysis through analyzing the levels of labeled TCA cycle intermediates by GC-MS. Data are shown as mean ± SD; n = 4 biological replicates for each condition/genotype; p values were calculated by two-way ANOVA, followed by Tukey.

e, f AMPK-PDZD8-GLS1 axis promotes pharyngeal pumping rates in nematodes. Experiments were performed as in Fig. 1m (**e**) and 1n (**f**), respectively, except that nematodes were treated with 2-DG for 2 days. Data are shown as mean ± SD; n = 10 for each condition/genotype. p values were calculated by two-way ANOVA, followed by Tukey.

g, h AMPK-PDZD8-GLS1 axis promotes resistance of nematodes to oxidative stress. Experiments were performed as in Fig. 1o (**g**) and 1p (**h**), respectively, except that nematodes were treated with 2-DG for 2 days before the FeSO₄ treatment. Experiments in this figure were performed three times.



Supplementary information, Fig. S3 PDZD8 exerts rejuvenating effects in nematodes

a, f AMPK-PDZD8 axis induces transient mitochondrial ROS and expression of ROS-depleting enzymes in low glucose. The *pdzd-8^{-/-}* nematodes with re-introduced PDZD8-T527A were treated with 2-DG for desired durations, followed by determination of mitochondrial ROS using the mitoSOX dye (**f**; data are shown as mean \pm SEM; $n = 10$ biological replicates for each condition). At 48 h after 2-DG treatment, an RNA-sequencing experiment was performed, and the mRNA levels of ROS-depleting enzymes are shown (**a**; data are shown as mean \pm SEM; $n = 4$ biological replicates for each condition/genotype). *p* values were determined by one-way ANOVA, followed by Dunn (WT nematodes of **f**) or Tukey (T527A nematodes of **f**), or by two-way ANOVA, followed by Tukey (**a**), all compared to the untreated group of each genotype.

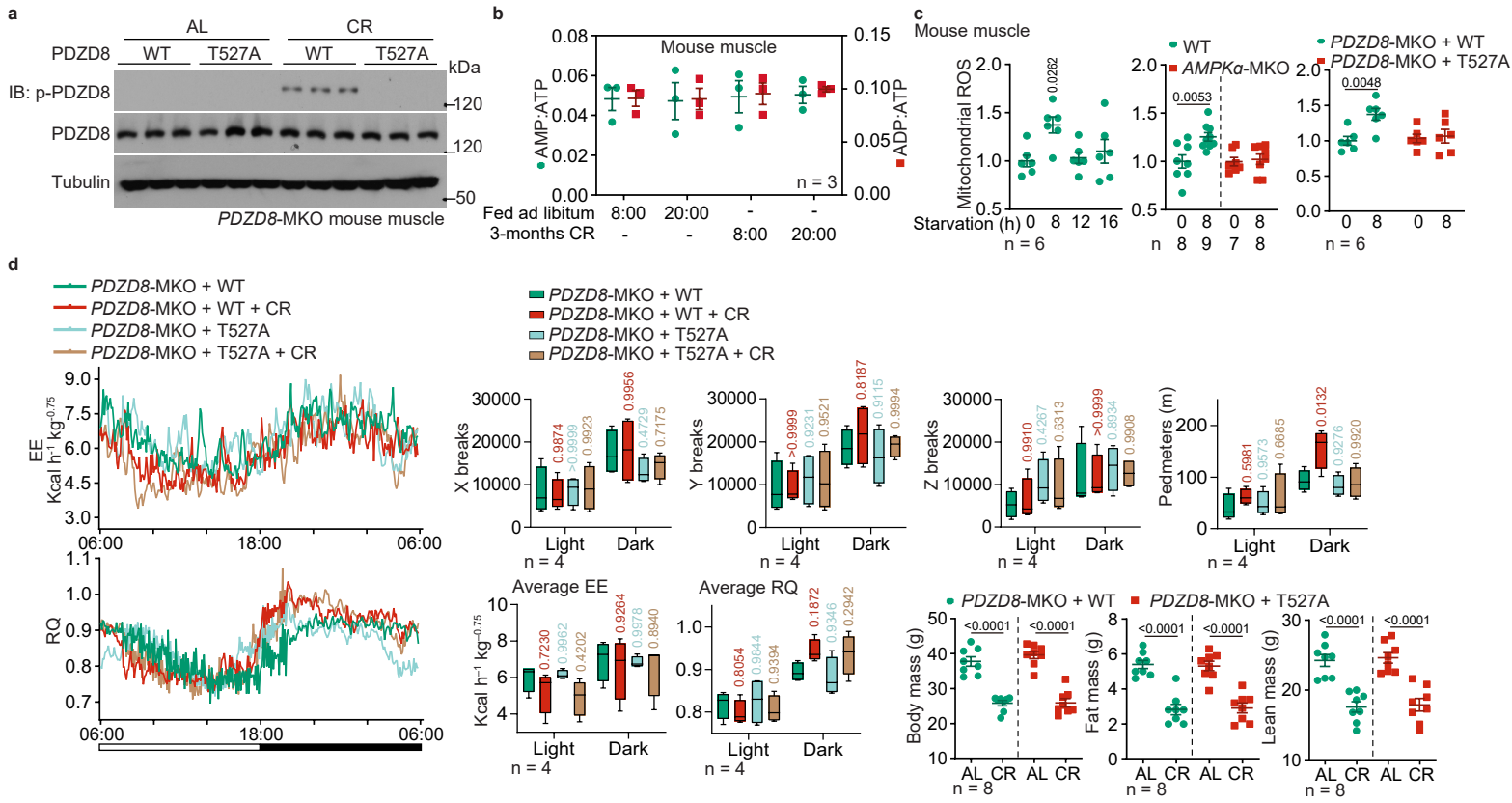
b, g AMPK-PDZD8 axis induces transient mitochondrial ROS and expression of ROS-depleting enzymes in nematodes subjected to CR for the desired duration (**g**, or 2 days in **b**). Experiments in (**g**) (data are shown as mean \pm SEM; with *n* values labeling on the panel) and (**b**) (data are shown as mean \pm SEM; $n = 4$ biological replicates for each condition/genotype) were performed as in **f** and **a**, except CR was applied. *p* values were determined by one-way ANOVA, followed by Dunn (WT nematodes of **g**) or Tukey (T527A nematodes of **g**), or by two-way ANOVA, followed by Tukey (**b**), all compared to the untreated group of each genotype.

c AMPK-PDZD8 axis is required for the increased expression of *sod-4*. The *pdzd-8^{-/-}* nematodes with re-introduced wildtype PDZD8 or PDZD8-T527A were treated with 2-DG for desired durations, followed by determination of mRNA levels of *sod-4* by RT-PCR. Data are shown as mean \pm SEM; $n = 3$ biological replicates for each condition/genotype. *p* values were calculated by one-way ANOVA, followed by Tukey, all compared to the untreated group of each genotype.

d, e GLS1 is required for the AMPK-PDZD8-induced transient mitochondrial ROS in nematodes. Experiments were performed as in **f** and **g**, respectively, except that the *glna*-depletion strain re-introduced with KGA-33A was used. Data are shown as mean \pm SD; *n* values are labeled on each panel. *p* values were calculated by two-way ANOVA, followed by Tukey, all compared to the untreated group of each genotype.

h Quenching of ROS burst in calorie-restricted nematodes prevents the induction of ROS-depleting enzymes. The N2 nematodes were subjected to CR and were treated with 5 mM NAC, as in Fig. 1q. The mRNA levels of *sod-4* were determined by RT-PCR. Data are shown as mean \pm SEM; $n = 3$ biological replicates for each condition. *p* values were calculated by one-way ANOVA, followed by Tukey.

Experiments in this figure were performed three times.



Supplementary information, Fig. S4 PDZD8 exerts rejuvenating effects in mice

a Validation of PDZD8 phosphorylation in the *PDZD8-MKO* mice with muscle-specific re-introduction of wildtype PDZD8 or PDZD8-T527A. Mice at 8 months were subjected to CR for another 3 months, followed by immunoblotting to determine PDZD8-phosphorylation in muscle tissues at 4 p.m. (1 h before the feeding time of each day during CR).

b CR does not elevate AMP levels in mouse muscle. *PDZD8-MKO* mice with muscle-specific re-introduction of wildtype PDZD8 were subjected to CR or fed ad libitum for 3 months, followed by determining the AMP:ATP and ADP:ATP ratios by CE-MS. Data are shown as mean \pm SEM; n = 3 mice for each condition; and p values were determined by one-way ANOVA, followed by Tukey.

c AMPK-PDZD8 axis induces transient mitochondrial ROS in mouse muscle. Wildtype mice (left panel), *AMPK α -MKO* mice (middle panel), or *PDZD8-MKO* mice with muscle-specific re-introduction of wildtype PDZD8 or PDZD8-T527A (right panel) were subjected to CR, followed by determination of muscle mitochondrial ROS using the mitoSOX dye at different starvation time points during the first day of CR. Data are shown as mean \pm SEM; n (labeled on each panel) values indicate biological replicates for each condition; and p values were determined by one-way ANOVA, followed by Tukey (left panel), unpaired two-tailed Student's *t*-test (middle panel), or two-way ANOVA, followed by Sidak (right panel).

d Muscle-specific re-introduction of PDZD8 does not affect body, fat and lean mass, pedestrial locomotion, or energy expenditure. Aged (8-month-old) *PDZD8-MKO* mice with muscle-specific re-introduction of wildtype PDZD8 or PDZD8-T527A were subjected to CR for 3 months, followed by determination of body weight, body composition (fat and lean mass), and energy expenditure (EE; see also respiratory quotient (RQ) and locomotion data). Data are shown as the mean \pm SEM (body weight and body composition), mean (EE curves; at 5-min intervals during a 24-h course after normalization to the body weight ($\text{kg}^{0.75}$), and RQ curves), or as box-and-whisker plot (average EE, average RQ, and locomotion, in which the lower and upper bounds of the box represent the first and the third quartile scores, the center line represents the median, and the lower and upper limits denote minimum and maximum scores, respectively); n = 4 (EE, RQ, and locomotion) or 8 (others) mice for each treatment; and p values were determined by one-way ANOVA, followed by Tukey (body, fat and lean mass), two-way ANOVA, followed by Sidak (average EE), or two-way ANOVA, followed by Dunnet (others).

Experiments in this figure were performed three times.

1 MATERIALS AND METHODS

2 Antibodies

3 Rabbit polyclonal antibody against p-T527-PDZD8 (1:1,1000 dilution for
4 immunoblotting (IB)) was raised and validated as described previously¹. Rabbit anti-
5 phospho-AMPK α -Thr172 (cat. #2535, RRID: AB_331250; 1:1,000 for IB), anti-
6 AMPK α (cat. #2532, RRID: AB_330331; 1:1,000 for IB), anti-phospho-AMPK
7 substrate motif (cat. #5759, RRID: AB_10949320; 1:1,000 for IB and 1:25 for
8 immunoprecipitation (IP)) anti-phospho-ACC-Ser79 (cat. #3661, RRID: AB_330337;
9 1:1,000 for IB), anti-ACC (cat. #3662, RRID: AB_2219400; 1:1,000 for IB), anti-Myc-
10 tag (cat. #2278, RRID: AB_490778; 1:1,000 for IB and 1:100 for IP), horseradish
11 peroxidase (HRP)-conjugated mouse anti-rabbit IgG (conformation-specific, cat.
12 #5127, RRID: AB_10892860; 1:2,000 for IB), and mouse anti-Myc-tag (cat. #2276,
13 RRID: AB_331783; 1:500 for IB and 1:100 for IP) antibodies were purchased from
14 Cell Signaling Technology. Rabbit anti-PDZD8 (cat. NBP2-58671; 1:1,000 for IB) was
15 purchased from Novus Biologicals. Rabbit anti-tubulin (cat. 10068-1-AP, RRID:
16 AB_2303998; 1:1,000 for IB nematode tubulin) and mouse anti-tubulin (cat. 66031-1-
17 Ig, RRID: AB_11042766; 1:20,000 for IB mammalian tubulin) antibodies were
18 purchased from Proteintech. Mouse anti-MHCIIa (cat. SC71, RRID: AB_2147165;
19 1:100 for immunohistochemistry (IHC)), anti-MHCIIb (cat. BF-F3, RRID:
20 AB_2266724; 1:100 for IHC), and anti-MHCI (cat. C6B12, RRID: AB_528351; 1:100
21 for IHC) antibodies were purchased from Developmental Studies Hybridoma Bank.
22 HRP-conjugated goat anti-mouse IgG (cat. #115-035-003, RRID: AB_10015289;

23 1:5,000 for IB) and goat anti-rabbit IgG (cat. #111-035-003, RRID: AB_2313567;

24 1:5,000 for IB) antibodies were purchased from Jackson ImmunoResearch.

25

26 **Chemicals and assay kits**

27 Glucose (cat. G7021), DMSO (cat. D2650), PBS (cat. P5493), NaCl (cat. S7653),

28 NaOH (cat. S8045), HCl (cat. 320331), agar (cat. A1296), CaCl₂ (cat. C5670), MgSO₄

29 (cat. M2643), KH₂PO₄ (cat. P5655), K₂HPO₄ (cat. P9666), cholesterol (cat. C3045),

30 Na₂HPO₄ (cat. S7907), NaH₂PO₄ (cat. S8282), sodium hypochlorite solution (NaClO;

31 cat. 239305), HEPES (cat. H4034), EDTA (cat. E6758), EGTA (cat. E3889), MgCl₂

32 (cat. M8266), CsCl (cat. 289329), ethanol (cat. 459836), isopropanol (cat. 34863),

33 glycerol (cat. G5516), IGEPAL CA-630 (NP-40, cat. I3021), Triton X-100 (cat. T9284),

34 Tween-20 (cat. P9416), dithiothreitol (DTT; cat. 43815), IPTG (cat. I6758),

35 carbenicillin (cat. C1613), streptomycin (for nematode culture; cat. 85886), Trioxsalen

36 (TMP; cat. T6137), 2-deoxy-D-glucose (2-DG; cat. D8375), ampicillin (cat. A9518),

37 kanamycin (cat. E004000), iron(II) sulfate heptahydrate (FeSO₄; cat. F8633), agarose

38 (cat. A9539), hexadimethrine bromide (polybrene; cat. H9268), triple-free DMEM (cat.

39 D5030), sodium palmitate (PA; cat. P9767), carnitine (cat. C0283), Trizma base (Tris;

40 cat. T1503), sodium pyrophosphate (cat. P8135), β-glycerophosphate (cat. 50020),

41 sodium azide (NaN₃; cat. S2002), oligomycin A (cat. 75351), FCCP (cat. C2920),

42 antimycin A (cat. A8674), rotenone (cat. R8875), myristic-d27 acid (cat. 68698), BSA

43 (cat. A2153), methoxyamine hydrochloride (cat. 89803), MTBSTFA (with 1% t-

44 BDMCS; cat. M-108), pyridine (cat. 270970), methanol (cat. 646377), chloroform (cat.

45 C7559), ammonium acetate (cat. 73594), ammonium hydroxide solution (cat. 338818),
46 LC-MS-grade water (cat. 1153332500), mannitol (cat. M4125), L-methionine sulfone
47 (cat. M0876), D-campher-10-sulfonic acid (cat. 1087520), 3-aminopyrrolidine
48 dihydrochloride (cat. 404624), N,N-diethyl-2-phenylacetamide (cat. 384011), trimesic
49 acid (cat. 482749), diammonium hydrogen phosphate (cat. 1012070500), ammonium
50 trifluoroacetate (cat. 56865), FCCP (cat. C2920), and NAC (N-acetylcysteine; cat.
51 A9165) were purchased from Sigma. Penicillin-streptomycin (for DMEM preparation;
52 cat. 15140163), TRIzol (cat. 15596018), UltraPure DNase/RNase-Free Distilled Water
53 (RNase-free water; cat. 10977015), Maxima SYBR Green/ROX qPCR master mix (cat.
54 K0223), RNase-free DNase I (cat. EN0523), Qubit RNA BR assay kit (cat. Q10211),
55 Collibri Stranded RNA Library Prep Kit (cat. A39003024), Collibri Library
56 Quantification Kit (cat. A38524100), DMEM, high glucose (DMEM; cat. 11965175),
57 glucose-free DMEM (cat. 11966025), FBS (cat. 10099141C), Lipofectamine 2000 (cat.
58 11668500), MEM non-essential amino acids solution (cat. 11140050), GlutaMAX (cat.
59 35050061), sodium pyruvate (cat. 11360070), MitoSOX (cat. M36008), and Prestained
60 Protein MW Marker (cat. 26612) were purchased from Thermo Scientific.
61 Bacteriological peptone (cat. LP0137) was purchased from Oxoid. Seahorse XF base
62 medium (cat. 103334) and Seahorse XF Calibrant solution (cat. 100840) were
63 purchased from Agilent. O.C.T. Compound (cat. 4583) was purchased from Sakura
64 Finetek USA, Inc. PrimeSTAR HS polymerase (cat. R40A) was purchased from Takara.
65 Polyethylenimine (PEI; cat. 23966) was purchased from Polysciences. Nonfat dry milk
66 (cat. #9999) and normal goat serum (NGS; cat. #5425) were purchased from Cell

67 Signaling Technology. ReverTra Ace qPCR RT master mix with a gDNA Remover kit
68 was purchased from TOYOBO. Protease inhibitor cocktail (cat. 70221) and KAPA
69 HyperPure magnetic beads (cat. KK8010) were purchased from Roche. WesternBright
70 ECL and peroxide solutions (cat. 210414-73) were purchased from Advansta. [U-¹³C]-
71 glutamine (cat. 184161-19-1) was purchased from Cambridge Isotope Laboratories.
72 The isotope-labeled AMP (cat. 123603801), ADP (cat. 129603601), and ATP (cat.
73 121603801) standards were purchased from Silantes. 3-hydroxynaphthalene-2,7-
74 disulfonic acid disodium salt (2-naphtol-3,6-disulfonic acid disodium salt; cat.
75 H949580) was purchased from Toronto Research Chemicals. Hexakis(1H,1H,3H-
76 perfluoropropoxy)phosphazene (hexakis(1H, 1H, 3H-tetrafluoropropoxy)phosphazene;
77 cat. sc-263379) was purchased from Santa Cruz Biotechnology. rProtein A Sepharose
78 Fast Flow (cat. 17127904) and Protein G Sepharose 4 Fast Flow (cat. 17061806) beads
79 were purchased from Cytiva.

80

81 **Mouse strains**

82 Protocols for all rodent experiments were approved by the Institutional Animal Care
83 and the Use Committee of Xiamen University (XMULAC20180028 and
84 XMULAC20220050). Wildtype C57BL/6J mice (#000664) were obtained from The
85 Jackson Laboratory. *PDZD8*-MKO mice with skeletal muscle-specific reintroduction
86 of *PDZD8* or its T527A mutant were generated as described previously¹.

87

88 The following ages of mice were used: 1) for analyzing ROS in mouse skeletal muscles:

89 wild-type, *AMPK α* -MKO, and *PDZD8*-MKO mice with or without wildtype *PDZD8*
90 or *PDZD8-T527A* re-introduced, aged 8 weeks; and 2) for determining rejuvenating
91 effects of CR: wild-type, and *PDZD8*-MKO mice with or without wildtype *PDZD8* or
92 *PDZD8-T527A* re-introduced, aged 32 weeks.

93

94 ***Caenorhabditis elegans* strains**

95 Nematodes (hermaphrodites) were maintained on NGM plates spread with *E. coli* OP50
96 as standard food². All worms were cultured at 20 °C. Wildtype (N2 Bristol), *aak-*
97 *2(ok524; aak-2^{-/-})*, and *CA-aak-2* (AGD467; ref. ³) strains were obtained from
98 *Caenorhabditis* Genetics Center, and *glna-1* (tm6647) and *glna-3* (tm8446) from
99 National BioResource Project (NBRP). See also the details of all the nematode strains
100 used in this study in Supplementary Information, Table S3. All mutant strains were
101 outcrossed 6 times to N2 before the experiments. Unless stated otherwise, worms were
102 maintained on nematode growth medium (NGM) plates (1.7% (w/v) agar, 0.3% (w/v)
103 NaCl, 0.25% (w/v) bacteriological peptone, 1 mM CaCl₂, 1 mM MgSO₄, 25 mM
104 KH₂PO₄-K₂HPO₄, pH 6.0, 0.02% (w/v) streptomycin and 5 µg/mL cholesterol) spread
105 with *Escherichia coli* OP50 as standard food.

106

107 The *glna-1*-knockout and *glna-3*-knockout strains were crossed to generate a *glna-1*
108 and *glna-3* double knockout strain (as an example, and similar procedures were applied
109 to generate the *CA-aak-2;pdzd-8^{-/-}* strain). Before crossing, *glna-1*-knockout
110 hermaphrodites were synchronized: worms were washed off from agar plates with 15

111 mL M9 buffer (22.1 mM KH₂PO₄, 46.9 mM Na₂HPO₄, 85.5 mM NaCl and 1 mM
112 MgSO₄; final concentration, and same hereafter) supplemented with 0.05% (v/v) Triton
113 X-100 per plate, followed by centrifugation at 1,000× *g* for 2 min. The worm sediments
114 were suspended with 6 mL of M9 buffer containing 50% synchronizing bleaching
115 solution (by mixing 25 mL of NaClO solution (5% active chlorine), 8.3 mL of 25%
116 (w/v) NaOH, and 66.7 mL of M9 buffer, for a total of 100 mL), followed by vigorous
117 shaking for 2 min and centrifugation for 2 min at 1,000× *g*. The sediments were washed
118 twice with 12 mL of M9 buffer, then suspended with 6 mL of M9 buffer, followed by
119 rotating at 20 °C, 30 r.p.m. for 12 h. The synchronized worms were then transferred to
120 the NGM plate and cultured to the L4 stage, followed by heat-shocking at 28 °C for 12
121 h. The heat-shocked worms were then cultured at 20 °C for 4 days, and the males were
122 picked up for mating with *glna-1*-knockout hermaphrodites for another 36 h. The mated
123 hermaphrodites were transferred to new NGM plates and allowed to give birth to more
124 *glna-1*-knockout males for another 4 days at 20 °C. The *glna-1*-knockout males were
125 then picked up and co-cultured with *glna-3*-knockout hermaphrodites at a 1:2 ratio (e.g.,
126 4 males and 8 hermaphrodites on a 10-cm NGM plate) for mating for 36 h at 20 °C,
127 and the mated hermaphrodites (*glna-3*-knockout) were picked up for culturing for
128 another 2 days. The offspring were then picked up and individually cultured on the 35-
129 mm NGM plate, then individually subjected to genotyping after egg-laying (after
130 culturing for approximately 2 days). For genotyping, individual worms were lysed with
131 5 µl of Single Worm lysis buffer (50 mM HEPES, pH 7.4, 1 mM EGTA, 1 mM MgCl₂,
132 100 mM KCl, 10% (v/v) glycerol, 0.05% (v/v) NP-40, 0.5 mM DTT and protease

133 inhibitor cocktail). The lysates were then frozen at -80 °C for 12 h, then incubated at
134 65 °C for 1 h and 95 °C for 15 min on a thermocycler (XP Cyclor, Bioer). The lysates
135 were then cooled to room temperature, followed by amplifying genomic DNA on a
136 thermocycler with the following programs: pre-denaturing at 95 °C for 10 min;
137 denaturing at 95 °C for 10 s, then annealing and extending at 60 °C for 30 s in each
138 cycle; cycle number: 35. The following primer pairs were used for identifying the *glna-*
139 *1*-knockout: 5'-CCTGGACTGGGAATCGTTCA-3' and 5'-
140 TACAACTGCGAAACACCGAG-3'; and 5'-CCCTCATTATGCGAACGAAC-3' and
141 5'-CCCCCAGAAGTAGATAAACG-3' for identifying the *glna-3*-knockout. The
142 offspring generated from *glna-1*- and *glna-3*-knockout-assured individuals were then
143 outcrossed six times to the N2 strain.

144

145 The *glna-2* was then knocked down in the *glna-1* and *glna-3* double knockout strain
146 following the previously described procedures⁴. Briefly, synchronized worms (around
147 the L1 stage) were placed on the RNAi plates (NGM containing 1 mg/mL IPTG and 50
148 µg/mL carbenicillin) spread with HT115 *E. coli* stains containing RNAi against *glna-*
149 *2* (well L20 on plate II-5 from the Ahringer *C. elegans* RNAi Collection) for 2 days.
150 The knockdown efficiency was then examined by determining the levels of *glna-*
151 *2* mRNA by real-time quantitative PCR (qPCR). Approximately 1,000 worms were
152 washed off from an RNAi plate with 15 mL of M9 buffer containing Triton X-100,
153 followed by centrifugation for 2 min at 1,000× g. The sediment was washed twice with
154 1 mL of M9 buffer and then lysed with 1 mL of TRIzol. The worms were then frozen

155 in liquid nitrogen, thawed at room temperature, and then subjected to repeated freeze-
156 thaw for another two times. The worm lysates were then placed at room temperature
157 for 5 min, mixed with 0.2 mL of chloroform, followed by vigorous shaking for 15 s.
158 After 3 min, lysates were centrifuged at 20,000× g at 4 °C for 15 min, and 450 µl of the
159 aqueous phase (upper layer) was transferred to a new RNase-free centrifuge tube
160 (Biopur, Eppendorf), followed by mixing with 450 µl of isopropanol, then centrifuged
161 at 20,000× g at 4 °C for 10 min. The sediments were washed with 1 mL of 75% ethanol
162 (v/v) followed by centrifugation at 20,000× g for 10 min, then with 1 mL of anhydrous
163 ethanol followed by centrifugation at 20,000× g for 10 min. The sediments were then
164 dissolved with 20 µl of RNase-free water after evaporating the ethanol. The dissolved
165 RNA was then reverse-transcribed to cDNA using ReverTra Ace qPCR RT master mix
166 with a gDNA Remover kit, followed by performing real-time qPCR using Maxima
167 SYBR Green/ROX qPCR master mix on a CFX96 thermocycler (Bio-Rad) with the
168 programs as described in genotyping the *glna*-knockout strain. Data were analyzed
169 using CFX Manager software (v.3.1, Bio-Rad). Knockdown efficiency was evaluated
170 according to the CT value obtained. The primers for *glna-2* are 5'-
171 ACTGTTGATGGTCAAAGGGCA-3' and 5'-CTTGGCTCCTGCCCAACATA-3'.
172 The primers for *ama-1* (the internal control) are 5'-GACATTTGGCACTGCTTTGT-3'
173 and 5'-ACGATTGATTCCATGTCTCG-3'.
174
175 The *pdzd-8*^{-/-} nematode strains expressing human PDZD8 or its T527A mutant were
176 established following the methods described previously⁴, with minor modifications: a)

177 PDZD8-WT or its T527A mutant was first introduced to the N2 strain; b) such
178 generated strains were then subjected to knock out of the *pdzd8* gene; and c) the *pdzd8*-
179 knockout worms were then picked up for the further outcrossing with N2 strain. Briefly,
180 to generate an N2 strain expressing PDZD8 or its T527A mutant, cDNA of PDZD8 or
181 PDZD8-T527A mutant was inserted into a pJM1 vector, with GFP as a selection marker
182 between the *Nhe* I and *Kpn* I sites (expressed under control by a *sur-5* promoter), then
183 injected into the syncytial gonad of the worm (200 ng/ μ L, 0.5 μ L per worm). The
184 injected worms were then recovered on an NGM plate for 2 days, and the F₁ GFP-
185 expressing hermaphrodites were selected for further culture. The extrachromosomally
186 existing PDZD8 or PDZD8-T527A expression plasmid was then integrated into the
187 nematode genome using UV irradiation to establish nonmosaic transgenic strains
188 described previously⁵, with minor modifications. Briefly, 70 PDZD8 or PDZD8-T527A
189 mutant-expressing worms at the L4 stage were picked up and incubated with 600 μ L of
190 M9 buffer, followed by adding 10 μ L of TMP solution (3 mg/mL stock concentration
191 in DMSO) and rotating at 30 r.p.m. for 15 min in the dark. Worms were then transferred
192 to a 10-cm NGM plate without OP50 bacteria in the dark, followed by irradiating with
193 UV at a total dose of 35 J/cm² (exposed within 35 s) on a UV crosslinker (CL-508;
194 UVITEC). The irradiated worms were fed with 1 mL of OP50 bacteria at 10¹³/mL
195 concentration, and then cultured at 20 °C for 5 h in the dark, followed by individually
196 cultured on a 35-mm NGM plate for 1 week without transferring to any new NGM plate
197 (to make sure that F₁ was under starvation before further selection). The F₁ GFP-
198 expressing hermaphrodites were selected and individually cultured for another 2 days,

199 and those F₂ with 100% GFP-expressing hermaphrodites were selected for further
200 culture. The genomic sequence encoding *pdzd-8* was then knocked out from this strain
201 by injecting a mixture of a pDD122 (P_{eft-3}::Cas9 + ttTi5605 sgRNA) vector carrying
202 sgRNAs against *pdzd-8* (5'-GAGGATCGTATCCAGCATGG-3', and 5'-
203 GTGAGCACGAAGAAGCGTTG-3', designed using the CHOPCHOP
204 website <http://chopchop.cbu.uib.no/>), into young adult worms. The F₁ hermaphrodite
205 worms were individually cultured on an NGM plate. After egg-laying, worms were
206 lysed using Single Worm lysis buffer, followed by PCR with the programs as described
207 in genotyping the *glna*-knockout strain, except that the primers 5'-
208 ATCTCCACCACAAACATCACCT-3' and 5'-CTTCAAATGCTCGTCAGAGTG-3'
209 were used. The offspring generated from knockout-assured individuals were outcrossed
210 six times to the N2 strain. The *pdzd-8*^{-/-} nematode strains expressing human PDZD8-
211 T527D or PDZD8-T527E were generated as described above in a), except that PDZD8-
212 T527D or PDZD8-T527E were introduced to the N2 strain. The *aak-2*^{-/-} nematode
213 strains expressing human PDZD8, PDZD8-T527D, or PDZD8-T527E were generated
214 similarly, but using *aak-2*^{-/-} nematode as the background strain. Strains expressing
215 PDZD8, PDZD8-T527A, PDZD8-T527D, and PDZD8-T527E were determined to
216 express the various proteins at similar levels by immunoblotting and qPCR (performed
217 as described above, but using the primers 5'-AAGACCCGCTGATCGACTTC-3' and
218 5'-GTGTGCTTGCCTTGATGAT-3' to quantify the mRNA levels of PDZD8), were
219 chosen for further experiments. For all nematode experiments, worms at the L4 stage
220 were used, except those for CR 3 days after L4.

221

222 **Cell lines and viruses**

223 In this study, no cell line used is on the list of known misidentified cell lines maintained
224 by the International Cell Line Authentication Committee
225 (<https://iclac.org/databases/cross-contaminations/>). HEK293T cells (cat. CRL-3216)
226 were purchased from ATCC and were authenticated by STR sequencing. *PDZD8*^{-/-}
227 MEFs¹ and *AMPKα*^{-/-} HEK293T cells⁶ were generated and validated as described
228 previously. Cells were maintained in Dulbecco's modified Eagle's medium (DMEM)
229 supplemented with 10% fetal bovine serum (FBS), 100 IU penicillin, and 100 mg/mL
230 streptomycin at 37 °C in a humidified incubator containing 5% CO₂. Cells were verified
231 to be free of mycoplasma contamination. PEI at a final concentration of 10 μM was
232 used to transfect cells (for ectopic expression). The total DNA to be transfected for each
233 plate was adjusted to the same amount by using the relevant empty vector. Transfected
234 cells were harvested at 24 h after transfection.

235

236 Lentiviruses for stable expression (expressed at close-to-endogenous levels) were
237 packaged in HEK293T cells (in DMEM supplemented with 10% FBS and MEM non-
238 essential amino acids; approximately 2 mL) by transfection using Lipofectamine 2000.
239 At 30 h post-transfection, the medium was collected and centrifuged at 5,000× g for 3
240 min at room temperature. The supernatant was mixed with 10 μg/mL polybrene, and
241 was added to MEFs, followed by centrifugation at 3,000× g for 30 min at room
242 temperature (spinfection). Cells were incubated for another 24 h before further

243 treatments, and the expression levels of stably expressed protein were determined by
244 immunoblotting. In particular, for determining the expression levels of nematode pdzd-
245 8 and its S536A mutant in MEFs, qPCR was performed with the following primers: 5'-
246 CGAACACCGAATCTGTTGCC-3' and 5'- TTGAGGCACTCGAGCACTTT-3' for
247 *pdzd-8*, and 5'-GACTTCAACAGCAACTCCCAC-3' and 5'-
248 TCCACCACCCTGTTGCTGTA-3' for mouse *Gapdh*.

249

250 For glucose starvation, cells were rinsed twice with PBS, then incubated in glucose-
251 free DMEM supplemented with 10% FBS and 1 mM sodium pyruvate for desired
252 periods at 37 °C.

253

254 **Data reporting**

255 The chosen sample sizes were similar to those used in this field: n = 3-10 samples to
256 evaluate the levels of metabolites in tissues⁷⁻¹¹ and nematodes¹²⁻¹⁴; n = 3-9 samples to
257 determine OCR in tissues^{11,15} and nematodes¹⁶⁻¹⁸, and n = 6-10 samples to determine
258 mitochondrial ROS in tissues¹⁹ and nematodes^{20,21}; n = 3-4 samples to determine the
259 expression levels and phosphorylation levels of a specific protein in animal cells or
260 tissues²²; n = 3-4 samples to determine the mRNA levels of a particular gene²²; n = 200
261 worms were used to determine lifespan²³⁻²⁵; and n = 60 worms were used to determine
262 healthspan²⁶⁻²⁸. No statistical methods were used to predetermine the sample size. All
263 experimental findings were repeated as stated in figure legends, and all additional
264 replication attempts were successful. For animal experiments, mice or nematodes were

265 maintained under the same condition or place. For cell experiments, cells of each
266 genotype were cultured in the same CO₂ incubator and were parallel-seeded and
267 randomly assigned to different treatments. Each experiment was designed and
268 performed along with controls, and samples for comparison were collected and
269 analyzed under the same conditions. Randomization was applied wherever possible.
270 For example, during MS analyses for metabolites, samples were processed and applied
271 to the mass spectrometer in random orders. For animal experiments, sex-matched (only
272 for mice) and age-matched litter-mate animals in each genotype were randomly
273 assigned to different treatments. Otherwise, randomization was not performed. For
274 example, when performing immunoblotting, samples needed to be loaded in a specific
275 order to generate the final figures. Blinding was applied wherever possible. For
276 example, samples, cages, or agar plates during sample collection and processing were
277 labeled as code names that were later revealed by the individual who picked and treated
278 animals or cells but did not participate in sample collection and processing until
279 assessing the outcome. Similarly, during microscopy data collection and statistical
280 analysis, the fields of view were chosen on a random basis, and were performed by
281 different operators, preventing potentially biased selection for desired phenotypes.

282

283 **CR treatments of mice**

284 Unless stated otherwise, mice were housed with free access to water and standard diet
285 (65% carbohydrate, 11% fat, 24% protein) under specific pathogen-free conditions. The
286 light was on from 8:00 to 20:00, with the temperature kept at 21-24 °C and humidity at

287 40-70%. Only male mice were used in the study, and male littermate controls were used
288 throughout the study. For CR, mice were individually caged for 1 month before
289 treatment; each mouse was fed 2.5 g of standard diet (70% of ad libitum food intake for
290 a mouse at 4 months old and above) at 5 p.m. each day;

291

292 **Determination of mouse running capacity and grip strength**

293 The maximal running capacity was determined as described previously²⁹, with minor
294 modifications. Briefly, mice were trained on Rodent Treadmill NG (UGO Basile, cat.
295 47300) at 10 m/min for 5 min for 2 days with a normal light-dark cycle, and tests were
296 performed during the dark period. Before the experiment, mice were fasted for 2 h. The
297 treadmill was set at a 15° incline, and the speed of the treadmill was set to increase in
298 a ramp mode (10 m/min for 10 min followed by an increase to a final speed of 18 m/min
299 within 15 min). Mice were considered exhausted and removed from the treadmill,
300 following the accumulation of 5 or more shocks (0.1 mA) per minute for two
301 consecutive minutes. The distances traveled were recorded as the running capacity.

302

303 Grip strength was determined on a grip strength meter (Ugo Basile, cat. 47200)
304 following the protocol described previously²⁸. Briefly, the mouse was held by its tail
305 and lowered (“landed”) until all four limbs grasped the T-bar connected to a digital
306 force gauge. The mouse was further lowered to the extent that the body was horizontal
307 to the apparatus and then slowly, steadily drawn away from the T-bar until all four limbs
308 were removed from the bar, which gave rise to the peak force in grams. Each mouse

309 was repeated 5 times with 5-min intervals between measurements.

310

311 **Determination of body composition**

312 Lean and fat body mass were measured by quantitative magnetic resonance (EchoMRI
313 -100H Analyzer; Echo Medical Systems) as described previously¹¹. Briefly, the system
314 was pre-calibrated with oil standard. Mice were individually weighed, inserted into a
315 restrainer tube, and immobilized by gently inserting a plunger. The mouse was then
316 positioned to a gesture that curled up like a donut, with its head against the end of the
317 tube. The body composition of each mouse was measured with two repeated runs, and
318 the average values were taken for further analysis.

319

320 **Determination of energy expenditure**

321 Mouse EE was determined by a metabolic cage system (Promethion Line, CAB-16-1-
322 EU; Sable Systems International) as described previously³⁰. Briefly, the system was
323 maintained in a condition identical to that for housing mice. Each metabolic cage in the
324 16-cage system consisted of a cage with standard bedding, a food hopper, and a water
325 bottle connected to load cells for continuous monitoring. To minimize the stress of a
326 new environment, mice were acclimatized for 1 week before data collection. Mice
327 subjected to CR or ad libitum fed were randomly assigned/housed to prevent systematic
328 errors in measurement. Body weights and fat proportion of mice were determined
329 before and after the acclimation and the food and water intake daily. Mice found not
330 acclimatized to the metabolic cage (for example, resistance to eating and drinking) were

331 removed from the study. Data acquisition (5-min intervals for each cage) and instrument
332 control were performed using MetaScreen software (v.2.3.15.12, Sable Systems), and
333 raw data were processed using Macro Interpreter (v.2.32, Sable Systems). Ambulatory
334 activity and position were monitored using XYZ beam arrays with a beam spacing of
335 0.25 cm (beam breaks), and the mouse pedestrian locomotion (walking distance) within
336 the cage was calculated accordingly. Respiratory gases were measured using the GA-3
337 gas analyzer (Sable Systems) equipped with a pull-mode, negative-pressure system.
338 Airflow was measured and controlled by FR-8 (Sable Systems), with a set flow rate of
339 2,000 mL min⁻¹. Oxygen consumption (VO₂) and carbon dioxide production (VCO₂)
340 were reported in mL per minute. Water vapor was measured continuously, and its
341 dilution effect on O₂ and CO₂ was compensated mathematically in the analysis stream.
342 EE was calculated using the Weir equation: kcal
343 h⁻¹ = 60 × (0.003941 × VO₂ + 0.001106 × VCO₂). Differences in average EE were
344 analyzed by ANCOVA using body weight as the covariate. The RQ was calculated as
345 VCO₂/VO₂.

346

347 **Histology**

348 Muscle fiber types were determined as described previously^{31,32}. Briefly, mice were
349 sacrificed by cervical dislocation, and the muscle tissues were quickly excised,
350 followed by frozen in the isopentane (pre-chilled in liquid nitrogen) for 2 min (until
351 they appeared chalky white). The tissues were then quickly transferred to the
352 embedding molds containing O.C.T. Compound, and were frozen in liquid nitrogen for

353 another 10 min. The embedded tissues were then sectioned into 6- μ m slices at -20 °C
354 using a CM1950 Cryostat (Leica), followed by fixing in 4% paraformaldehyde for 10
355 min, and were then washed with PBS for 5 min at room temperature. After incubating
356 with PBST (PBS supplemented with 5% (v/v) Triton X-100) for 10 min, the sections
357 were blocked with BSA Solution (PBS containing 5% (m/v) BSA) for 30 min at room
358 temperature. Muscle fibers were stained with the antibody against MHCIIb (6 μ g/mL,
359 diluted in BSA Solution) overnight at 4 °C, followed by washing with PBS 3 times, 5
360 min each at room temperature. The sections were then incubated with Alexa Fluor 488-
361 conjugated, goat anti-mouse IgM antibody (1:200 diluted in BSA Solution) for 1 h at
362 room temperature in a dark humidified chamber, followed by washing with PBS for 3
363 times, 5 min each, incubated with 4% paraformaldehyde for 2 min, and then washed
364 with PBS twice, 5 min each, all at room temperature. The sections were then incubated
365 with antibody against MHCI (6 μ g/mL, diluted in BSA Solution) for 3 h at room
366 temperature in a dark humidified chamber, followed by washing with PBS buffer 3
367 times, 5 min each at room temperature, and then incubated with Alexa Fluor 594-
368 conjugated, goat anti-mouse IgG2b antibody (1:200 diluted in BSA Solution) for
369 another 1 h at room temperature in a dark humidified chamber, followed by washing
370 with PBS buffer for 3 times, 5 min each at room temperature. After fixing with 4%
371 paraformaldehyde for 2 min and washing with PBS twice, 5 min each at room
372 temperature, the sections were incubated with the antibody against MHCIIa (6 μ g/mL,
373 diluted in BSA Solution) for 3 h at room temperature in a dark humidified chamber,
374 followed by washing with PBS buffer for 3 times, 5 min each at room temperature, and

375 then incubated in Alexa Fluor 647-conjugated goat anti-mouse IgG1 antibody (1:200
376 diluted in BSA Solution) for another 1 h at room temperature in a dark humidified
377 chamber, followed by washing with PBS buffer for 3 times, 5 min each at room
378 temperature. Tissue sections were mounted with 90% glycerol and visualized on a Zeiss
379 LSM980 microscope.

380

381 **Evaluation of nematode lifespan and healthspan**

382 To determine the lifespan of nematodes, the synchronized worms were cultured to the
383 L4 stage before being transferred to the desired agar plates for determining lifespan.
384 For 2-DG or NAC treatment, 4 mM 2-DG or 4 mM NAC was freshly dissolved in water
385 and added to warm NGM supplemented with 1.7% (w/v) agar before pouring to make
386 the NGM plates. The plates were stored at 20 °C. For CR, OP50 bacteria were diluted
387 to the concentration of 10^9 /mL (along with 10^{12} /mL as the control, ad libitum fed group;
388 see ref. ³³). The diluted bacteria were isopycnically spread on the NGM plates (for a
389 35-mm NGM plate, 250 μ L of bacteria were used) containing 50 mg/L ampicillin and
390 50 mg/L kanamycin. Worms were transferred to new plates every 2 d. Live and dead
391 worms were counted during the transfer. Worms that displayed no movement upon
392 gentle touching with a platinum picker were judged dead. Kaplan-Meier curves were
393 graphed by Prism 9 (GraphPad Software), and the statistical analysis data was analyzed
394 using SPSS 27.0 (IBM).

395

396 Pharyngeal pumping rates, assessed as the numbers of contraction-relaxation cycles of

397 the terminal bulb on the nematode pharynx within 1 min, were determined as described
398 previously³⁴, with minor modification. Briefly, worms were treated with 2-DG or
399 subjected to CR for 2 days, followed by being picked and placed on a new NGM plate
400 containing *E. coli*. After 10 min of incubation at room temperature, the contraction-
401 relaxation cycles of the terminal bulb of each worm were recorded on a
402 stereomicroscope (M165 FC, Leica) through a 63× objective for a consecutive 4 min
403 using the Capture software (v.2021.1.13, Capture Visualization), and the average
404 contraction-relaxation cycles per min were calculated using the Aimersoft Video Editor
405 software (v.3.6.2.0, Aimersoft).

406

407 The resistance of nematodes to oxidative stress was determined as described
408 previously²⁶. Briefly, worms were treated with 2-DG or subjected to CR for 2 days.
409 Some 20 worms were then transferred to an NGM plate containing 15 mM FeSO₄.
410 Worms were then cultured at 20 °C on such a plate, during which the live and dead
411 worms were counted every 1 h.

412

413 **Determination of mRNA levels of antioxidative genes in nematodes**

414 Levels of antioxidative gene expression were determined through the RNA-sequencing
415 performed by Seqhealth Technology Co., Ltd. (Wuhan, China). Briefly, RNAs from
416 approximately 1,000 worms (treated with 2-DG, or undergone CR) were extracted as
417 described in the section of determining the knockdown efficiency of *glna-2*. The
418 residual DNA in each sample was removed by treating with RNase-free DNase I for 30

419 min at 37 °C, and the quality of RNA was double-checked through agarose gel (1.5%)
420 electrophoresis and the NanoDrop OneC Microvolume UV-Vis Spectrophotometer
421 (Thermo), followed by quantified on a Qubit 3 Fluorometer after staining with the Qubit
422 RNA BR kit. Some 2 µg of total RNAs were then subjected to construct cDNA libraries
423 using the Collibri Stranded RNA Library Prep Kit for Illumina Systems, following the
424 manufacturer's instructions. The cDNAs in the library with a length of 200-500 bps
425 were enriched using KAPA HyperPure magnetic beads following the manufacturer's
426 instructions, followed by quantification using the Collibri Library Quantification Kit,
427 and sequenced on a DNBSEQ-500 sequencer (MGI Tech Co., Ltd.) under the PEI150
428 mode. The low-quality sequences, including a) reads containing more than 50% bases
429 with quality lower than 20 in a sequence; b) reads with more than 5% bases unknown;
430 and c) reads containing adaptor sequences were removed from the total reads using the
431 Trimmomatic (version 0.36) software as described previously³⁵.

432

433 Expression levels of the antioxidative gene were quantified through their RPKM (reads
434 per kilobase of transcript per million reads mapped) values. To acquire the RPKM value
435 of each gene, reads were first mapped to the reference sequence of *C. elegans* using the
436 STAR software (version 2.5.3a) as described previously³⁶ to make sure that reads could
437 be uniquely mapped to the gene chosen to calculate the RPKM values. For genes with
438 more than one alternative transcript, the longest transcript was selected to calculate the
439 RPKM. The RPKM was calculated by the featureCounts software (version 1.5.1) as
440 described previously³⁷. RPKM values for each antioxidative gene were plotted using

441 Prism 9 (GraphPad) software.

442

443 In particular, to determine the mRNA levels of *sod-4* in nematodes, RT-PCR was used.

444 Some 1,000 worms were collected with 15 mL of M9 buffer containing 0.05% Triton

445 X-100 (v/v), followed by centrifugation for 2 min at 1,000× g. The sediment was then

446 washed with 1 mL of M9 buffer twice and then lysed with 1 mL of TRIzol. Worms were

447 then frozen in liquid nitrogen, thawed at room temperature, and then repeated freeze-

448 thaw for another 2 times. The worm lysates were then placed at room temperature for

449 5 min, then mixed with 0.2 mL of chloroform, followed by vigorous shaking for 15 s.

450 After centrifugation at 12,000× g for 15 min at 4 °C, 450 µL of each upper aqueous

451 layer was transferred to an RNase-free tube. The RNA was then precipitated by adding

452 450 µL of isopropanol, followed with centrifugation at 12,000× g for 30 min at 4 °C.

453 The pellet was washed twice with 75% ethanol, once with 100% ethanol, and dissolved

454 with 20 µL of DEPC-treated water. The concentration of RNA was determined by a

455 NanoDrop 2000 spectrophotometer (Thermo). Some 1 µg of RNA was diluted with

456 DEPC-treated water to a final volume of 10 µL, heated at 65 °C for 5 min, and chilled

457 on ice immediately. The Random Primer Mix, Enzyme Mix and 5× RT buffer (all from

458 the ReverTra Ace qPCR RT Kit) were then added to the RNA solution, followed by

459 incubation at 37 °C for 15 min, and then at 98 °C for 5 min on a thermocycler. The

460 reverse-transcribed cDNA was quantified with Maxima SYBR Green/ROX qPCR

461 Master Mix on a LightCycler 480 II System (Roche) with the following programs: pre-

462 denaturing at 95 °C for 10 min; denaturing at 95 °C for 10 s, then annealing and

463 extending at 65 °C for 30 s in each cycle [determined according to the amplification
464 curves, melting curves, and bands on agarose gel of serial pilot reactions (in which a
465 serial annealing temperature was set according to the estimated annealing temperature
466 of each primer pair) of each primer pair, and same hereafter], for a total of 45 cycles.
467 Primer sequences are as follows: *C. elegans ama-1*, 5'-
468 GACATTTGGCACTGCTTTGT-3' and 5'-ACGATTGATTCCATGTCTCG-3'; *C.*
469 *elegans sod-4*, 5'-CGGCTTCCGGAGACACATTA-3' and 5'-
470 ACCACACTTCGGCCAATGAT -3'.

471

472 **Plasmids**

473 Full-length cDNAs used in this study were obtained either by PCR using cDNA from
474 MEFs or nematodes, or by purchasing from Origene or Sino Biological. Mutations of
475 PDZD8, GLS1, and pdzd-8 were performed by PCR-based site-directed mutagenesis
476 using PrimeSTAR HS polymerase. Expression plasmids for various epitope-tagged
477 proteins were constructed in the pcDNA3.3 vector (#K830001, Thermo) for
478 transfection (ectopic expression) in HEK293T cells, or in the pBOBI vector for
479 lentivirus packaging (stable expression) in HEK293T cells. PCR products were verified
480 by sequencing (Invitrogen, China). *Escherichia coli* strain DH5 α (cat. #PTA-1977) was
481 purchased from ATCC and was used to amplify plasmids. All plasmids used in this
482 study were purified using the CsCl density gradient ultracentrifugation method. The
483 expression plasmids constructed in this study have been deposited to Addgene
484 (https://www.addgene.org/Sheng-cai_Lin/).

485

486 **IP and IB assays**

487 To verify the phosphorylation of nematode pdzd-8 by AMPK (using the anti-pan-
488 phospho-AMPK substrate antibody), a 10 cm-dish of HEK293T cells was transfected
489 with Myc-tagged pdzd-8-expression plasmids. Cells were lysed with 1 mL of ice-cold
490 Triton lysis buffer (20 mM Tris-HCl, pH 7.5, 150 mM NaCl, 1 mM EDTA, 1 mM EGTA,
491 1% (v/v) Triton X-100, 2.5 mM sodium pyrophosphate, 1 mM β -glycerophosphate,
492 with protease inhibitor cocktail), followed by sonication and centrifugation at 4 °C for
493 15 min. Cell lysates were incubated with anti-Myc-tag (1:100) antibodies, along with
494 protein A/G beads (1:100 dilution, balanced with Triton lysis buffer), added into the
495 supernatant, and mixed for 15 min at 4 °C. The beads were washed with 200 times
496 volume of ice-cold Triton lysis buffer 3 times at 4 °C, mixed with an equal volume of
497 2 \times SDS sample buffer, and boiled for 10 min before immunoblotting.

498

499 To analyze the levels of p-PDZD8 muscle tissues, mice were anesthetized after
500 indicated treatments. Freshly excised (or freeze-clamped) tissues were immediately
501 lysed with ice-cold Triton lysis buffer (5 μ L/mg tissue weight), followed by
502 homogenized and centrifuged at 20,000 \times g for 10 min at 4 °C. The supernatant was
503 then mixed with an equal volume of 2 \times SDS sample buffer, followed by boiling for 10
504 min, and then directly subjected to immunoblotting. To analyze the levels of PDZD8 in
505 nematodes, about 150 nematodes cultured on the NGM plate were collected for each
506 sample. Worms were quickly washed with ice-cold M9 buffer containing Triton X-100,

507 and were lysed with 150 μ L of ice-cold Triton lysis buffer. The lysates were mixed with
508 5 \times SDS sample buffer, followed by homogenization and centrifugation as described
509 above, and then boiled before being subjected to immunoblotting. All samples were
510 subjected to immunoblotting on the same day of preparation, and any freeze-thaw
511 cycles were avoided.

512

513 For immunoblotting, the SDS-polyacrylamide gels were prepared in-house. The
514 thickness of the gels used in this study was 1.0 mm. Samples of less than 10 μ L were
515 loaded into wells, and the electrophoresis was run at 100 V (by PowerPac HC High-
516 Current Power Supply, Bio-Rad) in a Mini-PROTEAN Tetra Electrophoresis Cell (Bio-
517 Rad). In this study, all samples were resolved on 8% resolving gels, except the deletion
518 mutants of pdzd-8 (aa 1-256, 257-416, 870-1047, and 1048-1365) on 15%. The
519 resolved proteins were then transferred to the PVDF membrane (0.45 μ m, cat.
520 IPVH00010, Merck). The PVDF membrane was then blocked by 5% (w/v) BSA (for
521 all antibodies against phosphorylated proteins) or 5% (w/v) non-fat milk (for all
522 antibodies against total proteins) dissolved in TBST for 2 h on an orbital shaker at 60
523 rpm at room temperature, followed by rinsing with TBST for twice, 5 min each. The
524 PVDF membrane was then incubated with the desired primary antibody overnight at
525 4 $^{\circ}$ C on an orbital shaker at 60 rpm, followed by rinsing with TBST three times, 5 min
526 each at room temperature, and then the secondary antibodies for 3 h at room
527 temperature with gentle shaking. The secondary antibody was then removed, and the
528 PVDF membrane was further washed with TBST 3 times, 5 min each, at room

529 temperature. PVDF membrane was incubated in an ECL mixture (by mixing equal
530 volumes of ECL solution and Peroxide solution for 5 min), then life with Medical X-
531 Ray Film (FUJIFILM). The films were then developed with X-OMAT MX Developer
532 (Carestream) and X-OMAT MX Fixer and Replenisher solutions (Carestream) on a
533 Medical X-Ray Processor (Carestream) using Developer (Model 002, Carestream). For
534 re-probing, the PVDF membrane was boiled in water for 5 min, followed by washing
535 with TBST 3 times, 5 min each, at room temperature, and then incubated with desired
536 primary and secondary antibodies. The developed films were scanned using a
537 Perfection V850 Pro scanner (Epson) with an Epson Scan software (v.3.9.3.4), and were
538 cropped using Photoshop 2023 software (Adobe). Levels of total proteins and
539 phosphorylated proteins were analyzed on separate gels, and representative
540 immunoblots are shown. Uncropped immunoblots are uploaded as a “Full scans” file
541

542 **Determination of rates of glutaminolysis**

543 To determine the glutaminolysis rates in MEFs, cells from one 10-cm dish (60–70%
544 confluence) were collected for each measurement. MEFs were glucose-starved for
545 desired periods of time by incubating with triple-free (free of glucose, pyruvate, and
546 glutamine) DMEM supplemented with 4 mM glutamine, 1 mM sodium pyruvate, 100
547 μ M PA, 1 mM carnitine (according to ref. ³⁸), and 10% FBS. At 20 min before sample
548 collection, cells were incubated with pre-warmed triple-free DMEM supplemented with
549 3 mM glutamine, 1 mM [U-¹³C]-glutamine, 1 mM sodium pyruvate, 100 μ M PA, 1 mM
550 carnitine, and 10% FBS. To determine the rates of glutaminolysis in *C. elegans*, 1,000

551 nematodes were incubated with 8 mM [U-¹³C]-glutamine (final concentration, added to
552 a 6-cm NGM plate containing OP50 bacteria) for 24 h, followed by washing and
553 collecting with M9 buffer. Cells and worms were then lysed with 1 mL of 80% methanol
554 (v/v in water) containing 10 µg/mL myristic-d27 acid as an internal standard (IS),
555 followed by 20 s of vortex. After centrifugation at 15,000× g for 15 min at 4 °C, 600
556 µL of each supernatant (aqueous phase) was freeze-dried in a vacuum concentrator (a
557 LABCONCO #7310037 centrifuge connected to a LABCONCO #7460037 cold trap
558 and an EDWARDS nXDS15i pump) at 4 °C for 24 h. The lyophilized samples were
559 then subjected to derivatization by vortexing for 1 min after mixing each with 50 µL of
560 freshly prepared methoxyamine hydrochloride (20 mg/mL in pyridine), followed by
561 incubation at 4 °C for 1 h. The mixtures were sonicated at 0 °C by bathing in an ice
562 slurry for 10 min, and were then incubated at 37 °C for 1.5 h, followed by mixing with
563 50 µL of MTBSTFA and incubated at 55 °C for 1 h. Before subjecting to GC-MS,
564 samples were centrifuged at 15,000× g for 10 min, and some 60 µL of each supernatant
565 was loaded into an injection vial (cat. 5182-0714, Agilent; with an insert (cat. HM-1270,
566 Zhejiang Hamag Technology)) equipped with a snap cap (cat. HM-0722, Zhejiang
567 Hamag Technology). GC was performed on an HP-5MS column (30 m × 0.25 mm i.d.,
568 0.25 µm film thickness; cat. 19091S-433; Agilent) using a GC/MSD instrument (7890-
569 5977B, Agilent) as described previously¹¹. Briefly, the injector temperature of GC/MSD
570 was set at 260 °C. The column oven temperature was first held at 70 °C for 2 min, then
571 increased to 180 °C at the rate of 7 °C/min, then to 250 °C at 5 °C/min, then to 310 °C
572 at 25 °C/min, where it was held for 15 min. The MSD transfer temperature was 280 °C.

573 The MS quadrupole and source temperature were maintained at 150 °C and 230 °C,
574 respectively. Measurements were performed in both a scan mode (to assure the quality
575 and purity of each TCA cycle intermediate peak) and a selected ion monitoring (SIM)
576 mode (to maximize the sensitivity of GC-MS for quantifying each
577 metabolite/isotopomer). In SIM mode, the fragment ion with m/z values of $[M-57]$
578 (where M is the molecular mass of each derivatized metabolite, and the loss of the 57-
579 Da facile is attributed to the loss of the *tert*-butyl moiety of the metabolite in the GC of
580 each compound) was set as the quantitative ion. To ensure that all possible isotopomer
581 peaks, including those of naturally occurring isotopes of a specific metabolite (with n
582 carbon atoms), were recorded, the m/z values ranging from $[M-57]$ to $[M-57] + n + 1$
583 were included during the data collection. In particular, for pyruvate and α -KG, m/z
584 values from $[M-57]$ to $[M-57] + n + 2$ were recorded, owing to the oximation of these
585 two metabolites during the derivatization. The following m/z values were used for each
586 compound: 174, 175, 176, 177 and 178 for pyruvate; 289, 290, 291, 292 and 293 for
587 succinate; 287, 288, 289, 291 and 292 for fumarate; 346, 347, 348, 349, 350, 351 and
588 352 for α -KG; 419, 420, 421, 422 and 423 for malate; 418, 419, 420, 421 and 422 for
589 aspartate; 432, 433, 434, 435, 436 and 437 for glutamate; 431, 432, 433, 434, 435, 436
590 for glutamine; and 591, 592, 593, 594, 595, 596 and 597 for citrate. Data were collected
591 using the MassHunter GC/MS Acquisition software (v.B.07.04.2260, Agilent). For
592 quantification, peaks were extracted and integrated using GC-MS MassHunter
593 Workstation Qualitative Analysis software (v.B.07.01SP1, Agilent), and were corrected
594 for naturally occurring isotopes using the IsoCor software^{39,40} with the matrix-based

595 method.

596

597 **Determination of NAD⁺**

598 To determine levels of NAD⁺, high-performance liquid chromatography-mass
599 spectrometry (HPLC-MS) was performed¹¹. Briefly, some 50 mg of freshly excised
600 (using a freeze-clamp) muscle tissue was immediately frozen in liquid nitrogen, and
601 homogenized in 1 mL of ice-cold methanol. The lysates were then mixed with 1 mL of
602 chloroform and 400 μ L of water (containing 4 μ g/mL [U-¹³C]-glutamine as an IS),
603 followed by 20 s of vortexing. After centrifugation at 15,000 \times g for another 15 min at
604 4 °C, 800 μ L of the aqueous phase was collected, lyophilized in a vacuum concentrator
605 at 4 °C for 8 h, and then dissolved in 30 μ L of 50% (v/v, in water) acetonitrile, followed
606 by loading 20 μ L of solution into an injection vial (cat. 5182-0714, Agilent; with an
607 insert (cat. HM-1270, Zhejiang Hamag Technology)) equipped with a snap cap (cat.
608 HM-2076, Zhejiang Hamag Technology). Measurements were based on ref. ⁴¹ using a
609 QTRAP MS (QTRAP 5500, SCIEX) interfaced with a UPLC system (ExionLC AD,
610 SCIEX). Some 2 μ L of samples were loaded onto a HILIC column (ZIC-pHILIC, 5 μ m,
611 2.1 \times 100 mm, PN: 1.50462.0001, Millipore). The mobile phase consisted of 15 mM
612 ammonium acetate containing 3 mL/L ammonium hydroxide (>28%, v/v) in the LC-
613 MS grade water (mobile phase A) and LC-MS grade, 90% (v/v) acetonitrile in LC-MS
614 grade water (mobile phase B) run at a flow rate of 0.2 mL/min. Metabolites were
615 separated with the following HPLC gradient elution program: 95% B held for 2 min,
616 then 45% B in 13 min, held for 3 min, and then back to 95% B for 4 min. The mass

617 spectrometer was run on a Turbo V ion source in negative mode with a spray voltage
618 of -4,500 V. Source temperature was set at 550 °C, Gas No.1 at 50 psi, Gas No.2 at 55
619 psi, and curtain gas at 40 psi. Metabolites were measured using the multiple reactions
620 monitoring mode (MRM), and declustering potentials and collision energies were
621 optimized using analytical standards. The following transitions (parent ion/daughter ion)
622 were used for monitoring each compound: 662.0/540.1 for NAD⁺ and 149.9/114 for
623 [U-¹³C]-glutamine. Data were collected using Analyst software (v.1.7.1, SCIEX), and
624 the relative amounts of metabolites were analyzed using MultiQuant software (v.3.0.3,
625 SCIEX).

626

627 **Measurements of adenylates**

628 Levels of AMP, ADP, and ATP were analyzed by capillary electrophoresis-based mass
629 spectrometry (CE-MS) as described previously¹, with minor modifications. Briefly,
630 each measurement required 100 mg of muscle tissues. Muscle tissues were quickly
631 excised by freeze-clamping from anesthetized mice, followed by grinding in 1 mL of
632 methanol containing IS1 (50 μM L-methionine sulfone, 50 μM D-campher-10-sulfonic
633 acid, dissolved in water; 1:500 (v/v) added to the methanol and used to standardize the
634 metabolite intensity and to adjust the migration time). The lysate was then mixed with
635 1 mL of chloroform and 400 μL of water, followed by 20 s of vortexing. After
636 centrifugation at 15,000× g for 15 min at 4 °C, 450 μL of aqueous phase was collected
637 and was then filtrated through a 5-kDa cutoff filter (cat. OD003C34, PALL) by
638 centrifuging at 12,000× g for 3 h at 4 °C. In parallel, quality control samples were

639 prepared by combining 10 μL of the aqueous phase from each sample and then filtered
640 alongside the samples. The filtered aqueous phase was then freeze-dried in a vacuum
641 concentrator at 4 $^{\circ}\text{C}$, and then dissolved in 100 μL of water containing IS2 (50 μM 3-
642 aminopyrrolidine dihydrochloride, 50 μM N,N-diethyl-2-phenylacetamide, 50 μM
643 trimesic acid, 50 μM 2-naphthol-3,6-disulfonic acid disodium salt, dissolved in methanol;
644 used to adjust the migration time). A total of 20 μL of re-dissolved solution was then
645 loaded into an injection vial (cat. 9301-0978, Agilent; equipped with a snap cap (cat.
646 5042-6491, Agilent)). Before CE-MS analysis, the fused-silica capillary (cat.
647 TSP050375, i.d. 50 $\mu\text{m} \times 80$ cm; Polymicro Technologies) was installed in a CE/MS
648 cassette (cat. G1603A, Agilent) on the CE system (Agilent Technologies 7100). The
649 capillary was then pre-conditioned with Conditioning Buffer (25 mM ammonium
650 acetate, 75 mM diammonium hydrogen phosphate, pH 8.5) for 30 min, followed by
651 balanced with Running Buffer (50 mM ammonium acetate, pH 8.5; freshly prepared)
652 for another 1 h. CE-MS analysis was run at anion mode, during which the capillary was
653 washed by Conditioning Buffer, followed by injection of the samples at a pressure of
654 50 mbar for 25 s, and then separation with a constant voltage at -30 kV for another 40
655 min. Sheath Liquid (0.1 μM hexakis(1H, 1H, 3H-tetrafluoropropoxy)phosphazine, 10
656 μM ammonium trifluoroacetate, dissolved in methanol/water (50% v/v); freshly
657 prepared) was flowed at 1 mL/min through a 1:100 flow splitter (Agilent Technologies
658 1260 Infinity II; actual flow rate to the MS: 10 $\mu\text{L}/\text{min}$) throughout each run. The
659 parameters of the mass spectrometer (Agilent Technologies 6545) were set as: a) ion
660 source: Dual AJS ESI; b) polarity: negative; c) nozzle voltage: 2,000 V; d) fragmentor

661 voltage: 110 V; e) skimmer voltage: 50 V; f) OCT RFV: 500 V; g) drying gas (N₂) flow
662 rate: 7 L/min; h) drying gas (N₂) temperature: 300 °C; i) nebulizer gas pressure: 8 psig;
663 j) sheath gas temperature: 125 °C; k) sheath gas (N₂) flow rate: 4 L/min; l) capillary
664 voltage (applied onto the sprayer): 3,500 V; m) reference (lock) masses: m/z
665 1,033.988109 for hexakis(1H, 1H, 3H-tetrafluoropropoxy)phosphazine, and m/z
666 112.985587 for trifluoroacetic acid; n) scanning range: 50-1,100 m/z; and n) scanning
667 rate: 1.5 spectra/s. Data were collected using MassHunter LC/MS acquisition 10.1.48
668 (Agilent), and were processed using Qualitative Analysis B.06.00 (Agilent). The peak
669 areas of adenylates were calculated using the following parameters (m/z, retention time
670 (min)): a) AMP: 346.0558, 9.302; b) ADP: 426.0221, 10.930; and c) ATP: 505.9885,
671 11.848. Note that the retention time of each adenylate may vary between each run and
672 can be adjusted by isotope-labeled standards (dissolved in individual cell or tissue
673 lysates) run between each sample, so do IS1 and IS2.

674

675 **Determination of oxygen consumption rates**

676 The oxygen consumption rates (OCR) of MEFs were measured as described
677 previously¹. Briefly, cells were plated at 10,000 cells per well on a 96-well Seahorse
678 XF Cell Culture Microplate (Agilent) in full medium (DMEM containing 10% FBS)
679 overnight before the experiment, followed by glucose starvation for desired time
680 periods. Medium was then changed to Seahorse XF Base Medium supplemented with
681 10% FBS, 25 mM glucose (not included under starvation condition, and same hereafter),
682 4 mM glutamine (GlutaMAX) and 1 mM sodium pyruvate 1 h before the experiment.

683 Cells were then placed in a CO₂-free, XF96 Extracellular Flux Analyzer Prep Station
684 (Agilent) at 37 °C for 1 h. OCR was then measured at 37 °C in an XF96 Extracellular
685 Flux Analyzer (Agilent), with a Seahorse XFe96 sensor cartridge (Agilent) pre-
686 equilibrated in Seahorse XF Calibrant solution in a CO₂-free incubator at 37 °C
687 overnight. The assay was performed on a Seahorse XFe96 Analyzer (Agilent) at 37 °C
688 following the manufacturer's instruction. Concentrations of respiratory chain inhibitors
689 used during the assay were: oligomycin A at 10 μM, FCCP at 10 μM, antimycin A at 1
690 μM and rotenone at 1 μM (all final concentrations). Data were collected using Wave
691 2.6.1 Desktop software (Agilent) and exported to Prism 9 (GraphPad) for further
692 analysis according to the manufacturer's instructions.

693

694 The OCR of nematodes was measured as described previously⁴². Briefly, nematodes
695 were washed with M9 buffer for 3 times. Some 15 to 25 nematodes were then suspended
696 in 200 μL of M9 buffer, and were added to a well on a 96-well Seahorse XF Cell Culture
697 Microplate. The medium was then changed to Seahorse XF Base Medium
698 supplemented with 10% FBS, 25 mM glucose (not included under starvation condition,
699 and same hereafter), 4 mM glutamine (GlutaMAX), and 1 mM sodium pyruvate 1 h
700 before the experiment. Worms were then placed in a CO₂-free, XF96 Extracellular Flux
701 Analyzer Prep Station (Agilent) at 20 °C for 1 h. OCR was then measured at 20 °C in
702 an XF96 Extracellular Flux Analyzer (Agilent), with a Seahorse XFe96 sensor cartridge
703 (Agilent) pre-equilibrated in Seahorse XF Calibrant solution in a CO₂-free incubator at
704 20 °C overnight. The assay was performed on a Seahorse XFe96 Analyzer (Agilent) at

705 20 °C following the manufacturer's instruction. Concentrations of respiratory chain
706 inhibitors used during the assay were 10 µM FCCP and 40 mM sodium azide (final
707 concentrations). Data were collected using Wave 2.6.1 Desktop software (Agilent) and
708 exported to Prism 9 (GraphPad) for further analysis according to the manufacturer's
709 instructions. At the end of the assay, the exact number of nematodes in each well was
710 determined on a Cell Imaging Multi-Mode Reader (Cytation 1, BioTek) and was used
711 for normalizing/correcting OCR results.

712

713 **Determination of mitochondrial ROS**

714 For detecting the mitochondrial ROS levels in MEFs, cells were grown in 35-mm glass-
715 bottom dishes (cat. D35-20-10-N, In Vitro Scientific) to 50% confluence. Cells were
716 treated with 5 µM (final concentration) MitoSOX dye for 0.5 h at 37 °C, then washed
717 three times with 2 mL of pre-warmed culture medium, and incubated in fresh medium
718 containing ProLong™ Live Antifade Reagent before imaging. During imaging, live
719 cells were kept at 37 °C, 5% CO₂, in a humidified incubation chamber (Incubator PM
720 S1, Zeiss). Images were taken using an LSM 980 (Zeiss) with a 63× 1.4 NA oil objective,
721 during which a DPSS laser module (Lasos) at 594 nm was used to excite mitoSOX. The
722 parameters, including 'PMT voltage', 'Offset', 'Pinhole' and 'Gain', were kept
723 unchanged between each picture taken. The resolution of the image is 1,024×1,024
724 pixels. Images were processed and analyzed on Zen Blue 3.3 software (Zeiss), and
725 formatted on Photoshop 2023 software (Adobe).

726

727 For detecting the mitochondrial ROS levels in nematodes, synchronized nematodes
728 cultured to the L4 stage were treated with 2-DG or subjected to CR for 48 h. Nematodes
729 were then treated with 5 μ M (final concentration; added into the NGM plate containing
730 the OP50 bacteria) MitoSOX dye for another 12 h at 20 °C, followed by placing on the
731 center of an injection pad (prepared by placing 2 drops (approximately 50 μ L) of boiling
732 4% agarose (w/v) onto the center of a glass coverslip (24 \times 50 mm, 0.13–0.15 mm
733 thickness), immediately followed by flattening with another coverslip, then dried at
734 room temperature for 24 h). The pad was then subjected to imaging as described in
735 those of MEFs, except that an LSM 900 (Zeiss) with a \times 20, 0.8 NA plan-Apochromat
736 air objective was used, during which a laser module URGB (cat. 400102-9301-000,
737 Topica) using a 10-mW laser line at 561 nm was applied. Images were processed by
738 Zen 3.1 software (Zeiss), and formatted on Photoshop 2023 software (Adobe).

739

740 For detecting mitochondrial ROS levels in muscle tissues, mice were starved for desired
741 time periods, and were sacrificed by cervical dislocation. The gastrocnemius muscle
742 was then quickly excised and sliced to 0.05 cm³ cubes, followed by immediately
743 soaking in O.C.T. Compound at -20 °C for 20 min. The embedded tissues were then
744 sectioned into 15- μ m slices using a CM1950 Cryostat (Leica). Sections were stained
745 with 40 mL of 5 μ M (final concentration; by diluting the DMSO stock solution with
746 PBS) MitoSOX dye for 30 min at 37 °C in a Coplin jar, followed by washing for 3
747 times, 5 min each with 40 mL of PBS at room temperature. Sections were then mounted
748 with Antifade Mounting Medium, and were imaged on a DM4 B (Leica) microscope.

749

750 **Statistical analysis**

751 Statistical analyses were performed using Prism 9 (GraphPad Software), except for the
752 survival curves, which were analyzed using SPSS 27.0 (IBM). Each group of data was
753 subjected to the Kolmogorov-Smirnov test, Anderson-Darling test, D'Agostino-
754 Pearson omnibus test, or Shapiro-Wilk test for normal distribution when applicable. An
755 unpaired two-tailed Student's *t*-test was used to determine the significance between two
756 groups of normally distributed data. Welch's correction was used for groups with
757 unequal variances. An unpaired two-tailed Mann-Whitney test was used to determine
758 significance between data without a normal distribution. For comparisons between
759 multiple groups with one fixed factor, an ordinary one-way ANOVA was used, followed
760 by Tukey, Sidak, Dunnett, or Dunn as specified in the legends. The assumptions of
761 homogeneity of error variances were tested using F-test ($p > 0.05$). For comparison
762 between multiple groups with two fixed factors, an ordinary two-way ANOVA was used,
763 followed by Tukey's or Sidak's multiple comparisons test as specified in the legends.
764 Geisser-Greenhouse's correction was used where applicable. The adjusted means and
765 SEM, or SD, were recorded when the analysis met the above standards. Differences
766 were considered significant when $p < 0.05$, or $p > 0.05$, with large differences of
767 observed effects (as suggested in refs. ^{43,44}). Raw data and the statistical analysis data
768 are also provided in this study as a "Source data" file.

769

770 **References for Supplementary information**

771 1 Li, M. *et al.* AMPK targets PDZD8 to trigger carbon source shift from glucose
772 to glutamine. *Cell Res* (2024). <https://doi.org:10.1038/s41422-024-00985-6>

773 2 Brenner, S. The genetics of *Caenorhabditis elegans*. *Genetics* **77**, 71-94 (1974).

774 3 Mair, W. *et al.* Lifespan extension induced by AMPK and calcineurin is
775 mediated by CRTC-1 and CREB. *Nature* **470**, 404-408 (2011).
776 <https://doi.org:10.1038/nature09706>

777 4 Ma, T. *et al.* Low-dose metformin targets the lysosomal AMPK pathway
778 through PEN2. *Nature* (2022). <https://doi.org:10.1038/s41586-022-04431-8>

779 5 Han, M. *et al.* A Systematic RNAi Screen Reveals a Novel Role of a Spindle
780 Assembly Checkpoint Protein BuGZ in Synaptic Transmission in *C. elegans*.
781 *Front Mol Neurosci* **10**, 141 (2017). <https://doi.org:10.3389/fnmol.2017.00141>

782 6 Li, M. *et al.* Hierarchical inhibition of mTORC1 by glucose starvation-triggered
783 AXIN lysosomal translocation and by AMPK. *Life Metabolism* (2023).
784 <https://doi.org:10.1093/lifemeta/load005>

785 7 Zhang, C. S. *et al.* Fructose-1,6-bisphosphate and aldolase mediate glucose
786 sensing by AMPK. *Nature* **548**, 112-116 (2017).
787 <https://doi.org:10.1038/nature23275>

788 8 Zong, Y. *et al.* Hierarchical activation of compartmentalized pools of AMPK
789 depends on severity of nutrient or energy stress. *Cell Res* **29**, 460-473 (2019).
790 <https://doi.org:10.1038/s41422-019-0163-6>

791 9 Hui, S. *et al.* Glucose feeds the TCA cycle via circulating lactate. *Nature* **551**,
792 115-118 (2017). <https://doi.org:10.1038/nature24057>

- 793 10 Hui, S. *et al.* Quantitative Fluxomics of Circulating Metabolites. *Cell*
794 *metabolism* **32**, 676-688 e674 (2020).
795 <https://doi.org:10.1016/j.cmet.2020.07.013>
- 796 11 Zhang, C. S. *et al.* The aldolase inhibitor aloein mimics glucose starvation
797 to activate lysosomal AMPK. *Nat Metab* (2022).
798 <https://doi.org:10.1038/s42255-022-00640-7>
- 799 12 Perez, C. L. & Van Gilst, M. R. A ¹³C isotope labeling strategy reveals the
800 influence of insulin signaling on lipogenesis in *C. elegans*. *Cell metabolism* **8**,
801 266-274 (2008). <https://doi.org:10.1016/j.cmet.2008.08.007>
- 802 13 Falk, M. J. *et al.* Stable isotopic profiling of intermediary metabolic flux in
803 developing and adult stage *Caenorhabditis elegans*. *J Vis Exp* (2011).
804 <https://doi.org:10.3791/2288>
- 805 14 Vergano, S. S. *et al.* In vivo metabolic flux profiling with stable isotopes
806 discriminates sites and quantifies effects of mitochondrial dysfunction in *C.*
807 *elegans*. *Mol Genet Metab* **111**, 331-341 (2014).
808 <https://doi.org:10.1016/j.ymgme.2013.12.011>
- 809 15 Schuh, R. A., Jackson, K. C., Khairallah, R. J., Ward, C. W. & Spangenburg, E.
810 E. Measuring mitochondrial respiration in intact single muscle fibers. *Am J*
811 *Physiol Regul Integr Comp Physiol* **302**, R712-719 (2012).
812 <https://doi.org:10.1152/ajpregu.00229.2011>
- 813 16 Koopman, M. *et al.* A screening-based platform for the assessment of cellular
814 respiration in *Caenorhabditis elegans*. *Nature protocols* **11**, 1798-1816 (2016).

- 815 <https://doi.org:10.1038/nprot.2016.106>
- 816 17 Sarasija, S. & Norman, K. R. Measurement of Oxygen Consumption Rates in
817 Intact *Caenorhabditis elegans*. *J Vis Exp* (2019). <https://doi.org:10.3791/59277>
- 818 18 Ng, L. F. & Gruber, J. Measurement of Respiration Rate in Live *Caenorhabditis*
819 *elegans*. *Bio Protoc* **9**, e3243 (2019). <https://doi.org:10.21769/BioProtoc.3243>
- 820 19 Vaccaro, A. *et al.* Sleep Loss Can Cause Death through Accumulation of
821 Reactive Oxygen Species in the Gut. *Cell* **181**, 1307-1328 e1315 (2020).
822 <https://doi.org:10.1016/j.cell.2020.04.049>
- 823 20 Dingley, S. *et al.* Mitochondrial respiratory chain dysfunction variably increases
824 oxidant stress in *Caenorhabditis elegans*. *Mitochondrion* **10**, 125-136 (2010).
825 <https://doi.org:10.1016/j.mito.2009.11.003>
- 826 21 Yang, W. & Hekimi, S. A mitochondrial superoxide signal triggers increased
827 longevity in *Caenorhabditis elegans*. *PLoS Biol* **8**, e1000556 (2010).
828 <https://doi.org:10.1371/journal.pbio.1000556>
- 829 22 Zhang, C. S. *et al.* The lysosomal v-ATPase-Ragulator complex Is a common
830 activator for AMPK and mTORC1, acting as a switch between catabolism and
831 anabolism. *Cell Metab.* **20**, 526-540 (2014).
832 <https://doi.org:10.1016/j.cmet.2014.06.014>
- 833 23 Espada, L. *et al.* Loss of metabolic plasticity underlies metformin toxicity in
834 aged *Caenorhabditis elegans*. *Nat Metab* **2**, 1316-1331 (2020).
835 <https://doi.org:10.1038/s42255-020-00307-1>
- 836 24 Wu, L. *et al.* An Ancient, Unified Mechanism for Metformin Growth Inhibition

837 in *C. elegans* and Cancer. *Cell* **167**, 1705-1718 e1713 (2016).
838 <https://doi.org/10.1016/j.cell.2016.11.055>

839 25 Martin-Montalvo, A. *et al.* Metformin improves healthspan and lifespan in mice.
840 *Nat Commun* **4**, 2192 (2013). <https://doi.org/10.1038/ncomms3192>

841 26 De Rosa, M. J. *et al.* The flight response impairs cytoprotective mechanisms by
842 activating the insulin pathway. *Nature* **573**, 135-138 (2019).
843 <https://doi.org/10.1038/s41586-019-1524-5>

844 27 Yuan, J. *et al.* Two conserved epigenetic regulators prevent healthy ageing.
845 *Nature* **579**, 118-122 (2020). <https://doi.org/10.1038/s41586-020-2037-y>

846 28 Zhang, H. *et al.* NAD(+) repletion improves mitochondrial and stem cell
847 function and enhances life span in mice. *Science* **352**, 1436-1443 (2016).
848 <https://doi.org/10.1126/science.aaf2693>

849 29 Park, S. J. *et al.* DNA-PK Promotes the Mitochondrial, Metabolic, and Physical
850 Decline that Occurs During Aging. *Cell metabolism* **26**, 447 (2017).
851 <https://doi.org/10.1016/j.cmet.2017.07.005>

852 30 Liu, P. *et al.* Blocking FSH induces thermogenic adipose tissue and reduces
853 body fat. *Nature* **546**, 107-112 (2017). <https://doi.org/10.1038/nature22342>

854 31 Liu, L. *et al.* Histone methyltransferase MLL4 controls myofiber identity and
855 muscle performance through MEF2 interaction. *J Clin Invest* **130**, 4710-4725
856 (2020). <https://doi.org/10.1172/JCI136155>

857 32 Ham, D. J. *et al.* Distinct and additive effects of calorie restriction and
858 rapamycin in aging skeletal muscle. *Nat Commun* **13**, 2025 (2022).

- 859 <https://doi.org:10.1038/s41467-022-29714-6>
- 860 33 Greer, E. L. *et al.* An AMPK-FOXO pathway mediates longevity induced by a
861 novel method of dietary restriction in *C. elegans*. *Current biology : CB* **17**, 1646-
862 1656 (2007). <https://doi.org:10.1016/j.cub.2007.08.047>
- 863 34 Fang, E. F. *et al.* NAD(+) Replenishment Improves Lifespan and Healthspan in
864 Ataxia Telangiectasia Models via Mitophagy and DNA Repair. *Cell metabolism*
865 **24**, 566-581 (2016). <https://doi.org:10.1016/j.cmet.2016.09.004>
- 866 35 Bolger, A. M., Lohse, M. & Usadel, B. Trimmomatic: a flexible trimmer for
867 Illumina sequence data. *Bioinformatics* **30**, 2114-2120 (2014).
868 <https://doi.org:10.1093/bioinformatics/btu170>
- 869 36 Dobin, A. *et al.* STAR: ultrafast universal RNA-seq aligner. *Bioinformatics* **29**,
870 15-21 (2013). <https://doi.org:10.1093/bioinformatics/bts635>
- 871 37 Liao, Y., Smyth, G. K. & Shi, W. featureCounts: an efficient general purpose
872 program for assigning sequence reads to genomic features. *Bioinformatics* **30**,
873 923-930 (2014). <https://doi.org:10.1093/bioinformatics/btt656>
- 874 38 Vacanti, N. M. *et al.* Regulation of substrate utilization by the mitochondrial
875 pyruvate carrier. *Molecular cell* **56**, 425-435 (2014).
876 <https://doi.org:10.1016/j.molcel.2014.09.024>
- 877 39 Millard, P., Letisse, F., Sokol, S. & Portais, J. C. IsoCor: correcting MS data in
878 isotope labeling experiments. *Bioinformatics* **28**, 1294-1296 (2012).
879 <https://doi.org:10.1093/bioinformatics/bts127>
- 880 40 Millard, P., Letisse, F., Sokol, S. & Portais, J. C. Correction of MS data for

881 naturally occurring isotopes in isotope labelling experiments. *Methods Mol Biol*
882 **1191**, 197-207 (2014). https://doi.org:10.1007/978-1-4939-1170-7_12

883 41 Bajad, S. U. *et al.* Separation and quantitation of water soluble cellular
884 metabolites by hydrophilic interaction chromatography-tandem mass
885 spectrometry. *Journal of chromatography. A* **1125**, 76-88 (2006).
886 <https://doi.org:10.1016/j.chroma.2006.05.019>

887 42 Preez, G. D. *et al.* Oxygen consumption rate of *Caenorhabditis elegans* as a
888 high-throughput endpoint of toxicity testing using the Seahorse XF(e)96
889 Extracellular Flux Analyzer. *Scientific reports* **10**, 4239 (2020).
890 <https://doi.org:10.1038/s41598-020-61054-7>

891 43 Amrhein, V., Greenland, S. & McShane, B. Scientists rise up against statistical
892 significance. *Nature* **567**, 305-307 (2019). [https://doi.org:10.1038/d41586-019-](https://doi.org:10.1038/d41586-019-00857-9)
893 [00857-9](https://doi.org:10.1038/d41586-019-00857-9)

894 44 Wasserstein, R. L., Schirm, A. L. & Lazar, N. A. Moving to a World Beyond
895 “ $p < 0.05$ ”. *The American Statistician* **73**, 1-19 (2019).
896 <https://doi.org:10.1080/00031305.2019.1583913>

897